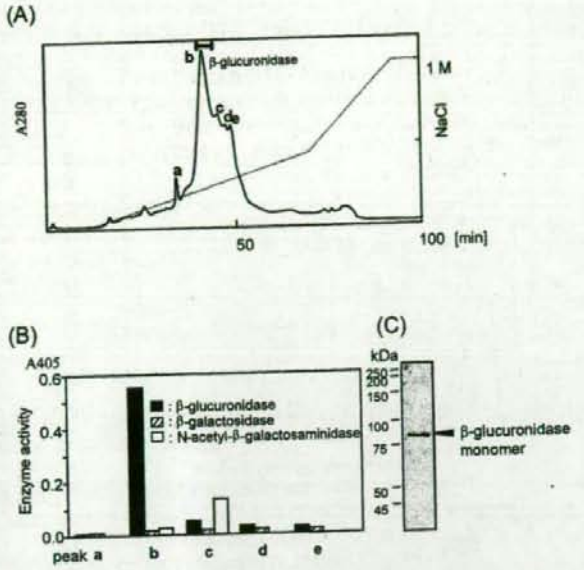

Fig. 4. Purification of fraction C by ion exchange high-performance liquid chromatography (HPLC). **(A)** The buffer C-eluted fraction from lactamyl affinity chromatography in Figure 3A was applied to ion-exchange HPLC on a DEAE-5PW column (21.5 × 150 mm, Tosoh Corp.). Elution was performed at a flow rate of 1.0 mL/min at room temperature with 10 mM TB (pH 7.5). After injection of the sample, the NaCl concentration was increased from 0 to 0.4 M, and then 0.4–1.0 M in 100 min. **(B)** Enzyme activities of each peak fraction. The peak fractions were pooled and measured for enzyme activity. Bars represent the activities of bovine liver β-glucuronidase (BLG) (■), β-D-galactosidase (▨), or *N*-acetyl-β-D-glucosaminidase (β-D-GlcNAcase) activities (□). **(C)** Sodium dodecyl sulfate–polyacrylamide gel electrophoresis (SDS–PAGE) of peak b under reducing conditions.

glycoproteins and lipids (data not shown). As shown in Figure 6A, immobilized BLG bound to asialofetuin better than fetuin and to asialoagalactofetuin but not to transferrin, asialotransferrin, ovalbumin, or BSM at pH7.5. It suggested that BLG recognized the exposed galactose residues of triantennary complex-type *N*-glycans but not the biantennary complex-type of asialotransferrin or the high Man or hybrid type of ovalbumin. BLG bound to lactosyl ceramide but not to Glc-cer, Gal-cer, ceramide, or sulfatide (Figure 6B). The direct binding of BLG to the sugar residues was demonstrated using sugar-BP probes. As shown in Figure 6C), BLG bound to *N*-acetyllactosamine-BP better than to the Lac-BP probe. Taken together, BLG was shown to bind to the *N*-acetyllactosamine or lactosyl sequence of glycoconjugates at neutral pH but not at pH 5.

Discussion

In this study, BLG was demonstrated for the first time to have binding activity toward lactose and *N*-acetyllactosamine sequences. BLG was effectively separated from contaminating glycosidases by affinity chromatography on a lactamyl–Sepharose column, and the specific activity was increased by 20-fold during one-step affinity chromatography (Table I). Non- or uncompetitive regulation of BLG with lactose indicated that the lactose-binding site is different from the substrate-binding site (Table III). Purified BLG bound best to the glycoconjugates possessing a nonreducing terminal *N*-acetyllactosamine/lactose such as asialofetuin and lactosylceramide (Figure 6), which is attributable to the carbohydrate-binding activity of BLG toward lactose/lactosamine structures.

Preparation of BLG has required multiple purification steps including heat denaturation of proteins (Ho, 1991), or fractionation with organic solvents (Himeno *et al.*, 1974), in combination with several chromatography steps to dissociate complex of BLG with other lysosomal proteins. This study provided convenient protocol to isolate BLG from other contaminating enzymes under mild conditions and

Table III. Effect of various sugars on bovine liver β-glucuronidase activity

Enzyme	Saccharide	Vmax	Kmapp	Mode of effect
Control		1.2×10^2	0.6	
Lactose	1 mM	2.0×10^2	0.6	Noncompetitive activation
	13 mM	1.5×10^2	1.1	Competitive inhibition
	130 mM	1.2×10^2	0.8	
Cellobiose	1 mM	1.3×10^2	0.6	
	10 mM	1.3×10^2	0.6	
	100 mM	1.4×10^2	0.6	
Melibiose	1 mM	1.4×10^2	0.6	
	13 mM	0.8×10^2	0.3	
	130 mM	0.8×10^2	0.4	
Saccharo-1,4-lactone	1 μM	1.2×10^2	2.0	Competitive inhibition
D-Glucuronic acid	1 mM	1.2×10^2	0.9	Competitive inhibition
Glc, Gal, GlcNAc, Man, maltose, Man-6P, NeuAc	No effect			

β-Glucuronidase activity was measured in the presence of free saccharide substrate concentrations (pH 5.0) of 0.1–1 mM and analyzed by a double reciprocal Lineweaver–Burk plot. Examples of the plots are shown in Figure 5.

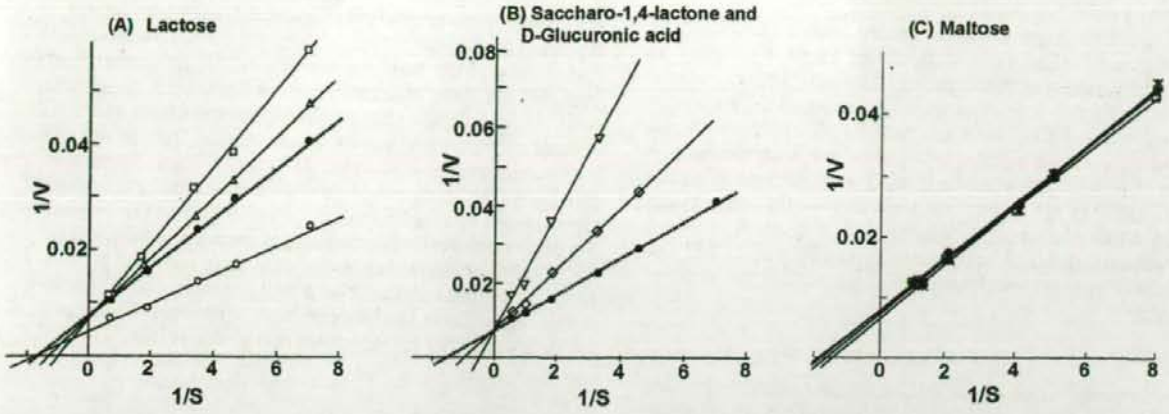

Fig. 5. Effect of free sugars on bovine liver β-glucuronidase (BLG) activity. Activity of BLG was measured using *p*-nitrophenyl-β-D-glucuronide as the substrate in the presence of various concentrations of sugars. (**A**) D-Lactose at (○) 1 mM, (□) 13 mM, and (△) 130 mM; (**B**) (▽) 1 μM Saccharo-1,4-lactone, or (◇) 1 mM D-glucuronic acid; (**C**) D-maltose at (□) 1 mM, (▲) 10 mM, (•) 100 mM, and (●) control without sugars.

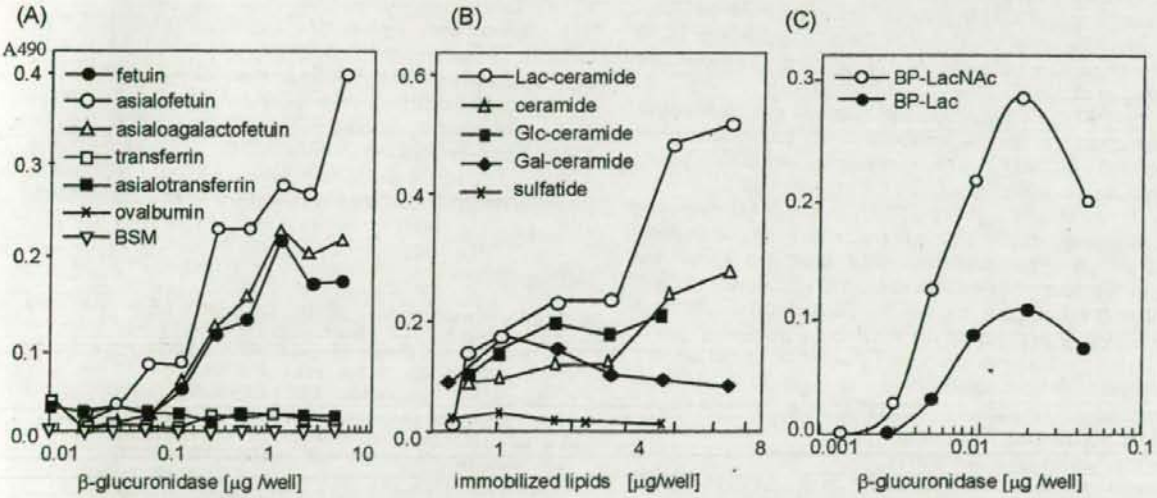

Fig. 6. Interaction of bovine liver β-glucuronidase (BLG) with biotinyl glycoproteins (**A**) and lipids (**B**) at pH7.5. (**A**) A solution of BLG was serially diluted in 10 mM Tris–HCl–150 mM NaCl (pH 7.5) (TBS) and immobilized on microtiter plates. Biotinyl glycoprotein probes were added to the wells, and a solid phase assay was performed as described in the text. Glycoproteins used were fetuin (—●—), asialofetuin (—○—), asialogalactofetuin (—△—), transferrin (—□—), asialotransferrin (—■—), ovalbumin (—×—) and BSM (—▽—). (**B**) Binding assay of biotinylated BLG to immobilized glycolipids. Lactosyl-ceramide (—○—), galactosyl-ceramide (—◆—), glucosyl-ceramide (—■—), ceramide (—△—), and sulfatide (—×—) were immobilized on microtiter plates with serial dilutions in methanol, respectively. Biotinylated BLG was added to the each well, and bound BLG was detected with ABC-HRP as described in the text. (**C**) BLG was immobilized at various concentrations on a microtiter plate, biotinyl polymer (BP)-sugar probes were added to the wells, and a solid phase assay was performed as described in the text. BP-LacNAc (—○—) and BP-Lac probes (—●—).

furthermore opens new insights into the biological functions of the carbohydrate-specific interaction of β-glucuronidase. The observations that BLG was eluted more effectively with GHAG than lactose and galactose from lactamyl–Sepharose column (Figure 2B), and BLG bound to *N*-acetyllactosamine-BP better than to the Lac-BP probe (Figure 6C) suggest the significance of *N*-acetyllactosamine structure present in the glycoconjugates as the biological ligand for BLG.

Interaction of BLG with carbohydrate ligands in lysosome

Although the lactamyl-binding activity of BLG was maximal at pH 6–7 and weakened to one-third at pH 5, the physiological pH of lysosomes (Figure 2), lactose noncompetitively activated BLG at 1 mM at pH 5, indicating that the carbohydrate-binding activity is exhibited even at pH 5. Therefore, the lactose binding may contribute to regulation of the enzyme activity in lysosomes. As a candidate for lysosomal ligands other than free lactose, BLG is supposed

to interact with lysosome-associated membrane glycoproteins 1 and 2 (Lamp1 and 2), major carriers for poly-*N*-acetyllactosamines (Laferte and Dennis, 1989), because the repeating *N*-acetyllactosamine sequence may enhance the affinity for BLG by a multivalent effect. However, we did not detect the binding of BLG to polylactosaminoglycans of human erythrocyte Band 3 glycoprotein (Fukuda *et al.*, 1984) at pH 5 (data not shown) by solid phase assay, while BLG did bind to it at pH 7 (Figure 6 and our unpublished data). Whether interaction between BLG and the glycoconjugates in lysosomes is possible is unknown at this point.

Biological function of the carbohydrate binding of BLG

Alternatively, the lactose/*N*-acetyllactosamine-binding activity may play a specific role at neutral pH in the endoplasmic reticulum (ER) and Golgi apparatus during glycoprotein maturation and in extracellular matrices after secretion. One possibility is that the lactose/*N*-acetyllactosamine-binding activity of BLG may be involved in the formation of the active tetrameric form because BLG contains a considerable amount of complex-type asialoglycans (Himeno *et al.*, 1974), and a wild-type BLG produced in the presence of tunicamycin was inactive (Shipley *et al.*, 1993).

In the ER and Golgi apparatus, various glycoconjugates are involved in the biosynthetic and lysosome-sorting processes of BLG. For example, phosphodiester α-GlcNAcase, which catalyzes the second step of attachment of the Man6P signal on BLG, is one of the *N*-glycosylated glycoproteins. The active site and the recognition motif of phosphotransferase have been elucidated on human β-glucuronidase (Jain *et al.*, 1996), but recognition motif of α-GlcNAcase has not yet been clarified. Because only a limited number of the α-GlcNAc phosphodiesters that are attached by GlcNAc-1-phosphotransferase are hydrolyzed by α-GlcNAcase to generate Man6P monoester (Natowicz *et al.*, 1982), the carbohydrate-binding activity of BLG could play a role in accessing phosphodiester α-GlcNAcase.

A carbohydrate-binding activity of a macromolecule-degrading enzyme might help localize the enzyme on an appropriate scaffold to exhibit catalytic action efficiently and stably *in vivo*. Lysosomal enzymes, including BLG, are released by the fusion of whole lysosomes with the plasma membrane into the synovial fluid in inflammatory joint diseases and in the invasion by metastatic tumor cells to focal dissolution of the extracellular matrix of surrounding tissues or penetration of endothelial membranes. (Sloane *et al.*, 1986; Andrei *et al.*, 2004). The observation that highly metastasizing tumor cells express more poly-*N*-acetyllactosamine in lysosomes than do their normal and poorly metastasizing counterparts (Dennis *et al.*, 1999, Chakraborty and Pawelek, 2003) supports the idea that the interaction of BLG with poly-*N*-acetyllactosamines may well be involved in concentrating the hydrolases and catalyzing the substrate hydrolysis efficiently at the cell surface when secreted outside the cell. A benefit for BLG of anchoring to poly-*N*-acetyllactosamines is cooperation with other hydrolases because the carbohydrate-binding activity is shared among several other lysosomal exoglycosidases, as shown in this study. β-GalNAcase and β-GlcNAcase exhibited considerable binding activity to affinity adsorbents immobilized with saccharides other than their substrates, such as galactose and tri*N*-acetylchitotriose (Table I). Several extracellular matrix glycoproteins that have polylactosaminoglycans, such as laminin, integrin, and neuronal glycoproteins, could provide a scaffold for lysosomal glycosidases secreted from tumor cells, so that the enzymes can act on substrates cooperatively. Such a hypothetical tie-up of glycan-degrading exoglycosidases on the poly-*N*-acetyllactosaminoglycan chain will increase the efficiency of the degradation of their common substrates. Those possibilities are under investigation in our laboratory.

Conflict of interest statement

None declared.

Abbreviations

BLG, bovine liver β-glucuronidase; BP, biotinyl polymer; GHAG, 1-deoxy-4-*o*-β-D-galactopyranosyl-1-[(2-hydroxyethyl)amino]-D-glucitol; HPLC, high-performance liquid chromatography; Me_2SO-d_6, $^2[CH_3]_2SO$; PAGE, polyacrylamide gel electrophoresis; SDS, sodium dodecyl sulfate; TBS, 10 mM Tris–HCl–150 mM NaCl (pH 7.5); X-, 5-bromo-4-chloro-3-indolyl-; β-D-GalNAcase, *N*-acetyl β-D-galactosaminidase; β-D-GlcNAcase, *N*-acetyl-β-D-glucosaminidase.

References

Andrei, C., Margiocco, P., Poggi, A., Lotti, L.V., Torrisi, M.R., and Rubartelli, A.T. (2004) Phospholipases C and A2 control lysosome-mediated IL-1 beta secretion: Implications for inflammatory processes. *Proc. Natl. Acad. Sci. U. S. A.*, **101**, 9745–9750.

Chakraborty, A.K. and Pawelek, J.M. (2003) GnT-V, macrophage and cancer metastasis: a common link. *Clin. Exp. Metastasis*, **20**, 365–373.

Davis, B.J. (1964) Disc electrophoresis. II. Method and application to human serum proteins. *Ann. N. Y. Acad. Sci.*, **121**, 404–427.

Dennis, J.W., Granovsky, M., and Warren, C.E. (1999) Glycoprotein glycosylation and cancer progression. *Biochim. Biophys. Acta*, **1473**, 21–34.

Fukuda, M., Dell, A. and Fukuda, M.N. (1984) Structure of fetal lactosaminoglycan. The carbohydrate moiety of Band 3 isolated from human umbilical cord erythrocytes. *J. Biol. Chem.* **259**, 4782–4791.

Harris, R.G., Rowe, J.J.M., Stewart, P.S., and Williams, D.C. (1973) Affinity chromatography of β-glucuronidase. *FEBS Lett.*, **29**, 189–192.

Himeno, M., Hashiguchi, Y., and Kato, K. (1974) β-Glucuronidase of bovine liver. Purification, properties, carbohydrate composition. *J. Biochem.*, **76**, 1243–1252.

Ho, K.J. (1991) A large-scale purification of β-Glucuronidase from human liver by immunoaffinity chromatography. *Biotechnol. Appl. Biochem.*, **14**, 296–305.

Holmes, E.W. and O'Brien, J.S. (1979) Separation of glycoprotein-derived oligosaccharides by thin-layer chromatography. *Anal. Biochem.*, **93**, 167–170.

Iida-Tanaka, N., Hikita, T., Hakomori, S., and Ishizuka, I. (2002) Conformational studies of a novel cationic glycolipid, glyceroplasmalopsychosine, from bovine brain by NMR spectroscopy. *Carbohydr Res.*, **337**, 1775–1779.

Iida-Tanaka, N. and Ishizuka, I. (2000) Complete ^1H and ^{13}C NMR assignment of mono-sulfated galactosylceramides with four types of ceramides from human kidney. *Carbohydr Res.*, **324**, 218–222.

Ito, Y., Seno, N., and Matsumoto, I. (1985) Immobilization of protein ligands on new formyl-spacer-carriers for the preparation of stable and high capacity affinity adsorbents. *J. Biochem.*, **97**, 1689–1694.

Jain, S., Drendel, W.B., Chen, Z.-w., Mathews, F.S., Sly, W.S., and Grubb, J.H. (1996) Structure of human β-glucuronidase reveals candidate lysosomal targeting and active-site motifs. *Nat. Struct. Biol.*, **3**, 375–381.

Kaplan, A. and Achord, D.T. (1977) Phosphohexosyl components of a lysosomal enzyme are recognized by pinocytosis receptors on human fibroblasts. *Proc. Natl. Acad. Sci. U. S. A.*, **74**, 2026–2030.

Kawai, Y. and Anno, K. (1971) Mucopolysaccharide-degrading enzymes from the liver of the squid, *Ommastrephes sloani pacificus*. I. Hyaluronidase. *Biochem. Biophys. Acta*, **242**, 428–436.

Kornfeld, S. (1987) Trafficking of lysosomal enzymes. *FASEB J.*, **1**, 462–468.

Kurtin, W.E. and Schwesinger, W.H. (1985) Assay of β-glucuronidase in bile following ion-pair extraction of pigments and bile acids. *Anal. Biochem.*, **147**, 511–516.

Laemmli, U.K. (1970) Cleavage of structural proteins during the assembly of the head of bacteriophage T4. *Nature*, **227**, 680–685.

Laferte, S. and Dennis, J.W. (1989) Purification of two glycoproteins expressing β1–6 branched Asn-linked oligosaccharides from metastatic tumour cells. *Biochem. J.*, **259**, 569–576.

Li, Y.T. and Li, S.C. (1972) α-Mannosidase, β-*N*-acetylhexosaminidase, and β-galactosidase from jack bean meal. *Meth. Enzymol.*, **28**, 702–713.

Matsumoto, I., Kitagaki, H., Akai, Y., Ito, Y., and Seno, N. (1981) Derivatization of epoxy-activated agrose with various carbohydrates for the preparation of stable and high-capacity affinity adsorbents. *Anal. Biochem.*, **116**, 103–110.

Natowicz, M., Baenziger, J.U., and Sly, W.S. (1982) Structural studies of the phosphorylated high mannose-type oligosaccharides on human β-glucuronidase. *J. Biol. Chem.*, **257**, 4412–4420.

Paigen, K. (1989) Mammalian β-glucuronidase: genetics, molecular biology, and cell biology. *Progr. Nucl Acid Res. Molec. Biol.*, **37**, 155–205.

Shipley, J.M., Grubb, J.H., and Sly, W.S. (1993) The role of glycosylation and phosphorylation in the expression of active human β-glucuronidase. *J. Biol. Chem.*, **268**, 12193–12198.

Sloane, B.F., Rozhin, J., Johnson, K., Taylor, H., Crissman, J.D., and Honn, K.V. (1986) Cathepsin B: association with plasma membrane in metastatic tumors. *Proc. Natl. Acad. Sci. U. S. A.*, **83**, 2483–2487.

Ueda, H., Saitoh, T., Kojima, K., and Ogawa, H. (1999) Multi-specificity of a *Psathyrella velutina* mushroom lectin: heparin/pectin binding occurs at a site different from the *N*-acetylglucosamine/*N*-acetylneuraminic acid-specific site. *J. Biochem.*, **126**, 530–537.

THE JOURNAL OF BIOLOGICAL CHEMISTRY VOL. 281, NO. 9, pp. 5484–5491, March 3, 2006

Structural Regions of MD-2 That Determine the Agonist-Antagonist Activity of Lipid IVa*

Received for publication, August 19, 2005, and in revised form, December 16, 2005 Published, JBC Papers in Press, December 31, 2005, DOI 10.1074/jbc.M509193200

Masashi Muroi and Ken-ichi Tanamoto[1]

From the Division of Microbiology, National Institute of Health Sciences, 1-18-1 Kamiyoga, Setagaya, Tokyo 158-8501, Japan

A cell surface receptor complex consisting of CD14, Toll-like receptor (TLR4), and MD-2 recognizes lipid A, the active moiety of lipopolysaccharide (LPS). *Escherichia coli*-type lipid A, a typical lipid A molecule, potently activates both human and mouse macrophage cells, whereas the lipid A precursor, lipid IVa, activates mouse macrophages but is inactive and acts as an LPS antagonist in human macrophages. This animal species-specific activity of lipid IVa involves the species differences in MD-2 structure. We explored the structural region of MD-2 that determines the agonistic and antagonistic activities of lipid IVa to induce nuclear factor-κB activation. By expressing human/mouse chimeric MD-2 together with mouse CD14 and TLR4 in human embryonic kidney 293 cells, we found that amino acid regions 57–79 and 108–135 of MD-2 determine the species-specific activity of lipid IVa. We also showed that the replacement of Thr^{57}, Val^{61}, and Glu^{122} of mouse MD-2 with corresponding human MD-2 sequence or alanines impaired the agonistic activity of lipid IVa, and antagonistic activity became evident. These mutations did not affect the activation of nuclear factor-κB, TLR4 oligomerization, and inducible phosphorylation of IκBα in response to *E. coli*-type lipid A. These results indicate that amino acid residues 57, 61, and 122 of mouse MD-2 are critical to determine the agonist-antagonist activity of lipid IVa and suggest that these amino acid residues may be involved in the discrimination of lipid A structure.

Bacterial lipopolysaccharide (LPS)[2] is a constituent of the outer membrane of the cell wall of Gram-negative bacteria and plays a major role in septic shock (1, 2). Engagement of LPS on the host cell results in rapid activation of a number of transcription factors, including NF-κB, which leads to production of inflammatory cytokines (3). Significant progress has been made in the identification of cell surface molecules that recognize LPS and transmit its signal to intracellular components. CD14, Toll-like receptor 4 (TLR4), and MD-2 participate in this molecular event and all of these molecules are necessary for cells to respond to picomolar concentrations of LPS (4, 5). A recent report (6) has suggested that sequential interactions of LPS with each of these molecules are required for optimal molecular recognition. LPS is first opsonized by the serum LPS-binding protein and then transferred to a CD14 molecule. This LPS-CD14 complex is further recognized by MD-2 to generate an LPS-MD-2 complex that produces TLR4-dependent cell stimulation. It has also been reported that MD-2 is necessary for TLR4 to undergo proper glycosylation and trafficking to the cell surface (7–9). Without MD-2, TLR4 is not able to reach the plasma membrane and resides predominantly in the Golgi apparatus. Thus, MD-2 is considered to play an important role for transferring LPS from CD14 to TLR4 and for correct cellular distribution of TLR4.

MD-2 also plays an important role for discriminating lipid A structure. The lipid A portion has been identified as the active center responsible for most LPS-induced biological effects (1, 10). *Escherichia coli*-type lipid A, a typical lipid A molecule, and its biosynthetic precursor lipid IVa have been synthesized chemically (compound 506 and 406, respectively), and their biological activities have been investigated extensively. Compound 506 and most varieties of LPS show little animal species-specific activity, whereas lipid IVa, as well as *Salmonella*-type lipid A, shows very little stimulatory activity and behaves as an antagonist in human macrophages, despite being potently active in murine macrophages (11, 12). This species-specific activity of lipid IVa and *Salmonella*-type lipid A has been attributed to the species difference in the structures of TLR4 (13, 14) and MD-2 (4, 15–17). Thus it is considered that MD-2 is also playing an important role for discriminating lipid A structure. To understand the molecular basis for this discriminating mechanism, we, in the present study, explored the structural region of MD-2 which determines the agonistic and antagonistic activities of lipid IVa.

EXPERIMENTAL PROCEDURES

Cell Culture and Reagents—The HEK293 cell line (obtained from the Human Science Research Resources Bank, Tokyo, Japan) was grown in Dulbecco's modified Eagle's medium (Invitrogen) supplemented with 10% (v/v) heat-inactivated fetal calf serum (Invitrogen), 100 units/ml penicillin, and 100 μg/ml streptomycin. Compound 506 and lipid IVa (compound 406) were obtained from Peptide Institute (Osaka, Japan). An antiserum against EIAV-tag epitope (amino acid sequence: ADRRIPGTAEE) was a kind gift from Dr. Nancy Rice (NCI-Frederick Cancer Research and Development Center). Stable transfectants expressing mouse CD14, EIAV-tagged mouse TLR4, FLAG-tagged mouse TLR4, and either EIAV-tagged mouse MD-2 or EIAV-tagged mouse MD-2-T57A,V61A,E122A were established as follows. After linearizing with PvuI, expression plasmids encoding the proteins described above were transfected into HEK293 cells by the calcium phosphate precipitation method. Stable transfectants were selected for G418 resistance at a concentration of 2 mg/ml. A monoclonal antibody (clone 5A5) that recognizes phosphorylated Ser^{32}-Ser^{36} of IκBα was purchased from Cell Signaling Technology (Danvers, MA).

Expression Plasmids—Expression plasmids encoding CD14, TLR4, and MD-2 as well as NF-κB-dependent luciferase reporter plasmid pELAM-L were described previously (16). Expression plasmids encoding MD-2 mutants were created by PCR-mediated mutagenesis, and mutations were confirmed by DNA sequencing.

NF-κB Reporter Assay—The NF-κB-dependent luciferase reporter assay was performed as described elsewhere (18). Briefly, HEK293 cells ($1–3 \times 10^5$/well) were plated in 12-well plates and on the following day

* This work was supported by a grant from the Ministry of the Environment. The costs of publication of this article were defrayed in part by the payment of page charges. This article must therefore be hereby marked "*advertisement*" in accordance with 18 U.S.C. Section 1734 solely to indicate this fact.

[1] To whom correspondence should be addressed. E-mail: tanamoto@nihs.go.jp.

[2] The abbreviations used are: LPS, lipopolysaccharide; HEK293, human embryonic kidney 293 cells; hMD-2, human MD-2; IκBα, inhibitor of NF-κB α; mMD-2, mouse MD-2; NF-κB, nuclear factor-κB; PBS, phosphate-buffered saline; TLR, Toll-like receptor.

transfected by the calcium phosphate precipitation method with 10 ng each of CD14, TLR4, and MD-2 mutant expression plasmids together with 0.1 μg of pELAM-L and 2.5 ng of phRL-TK (Promega, Madison, WI) for normalization. At 24 h after transfection, cells were stimulated for 6 h, and the reporter gene activity was measured according to the manufacturer's (Promega) instructions.

Detection of MD-2 Proteins Expressed on the Cell Surface—Detection of cell surface MD-2 was performed as described previously (19) with a slight modification. Briefly, HEK293 cells were plated in 6-cm dishes and transfected with indicated plasmids by the calcium phosphate precipitation method. After 24 h, the cells were transferred to 1.5-ml tubes and then washed twice with PBS. After suspension with 0.5 ml of PBS containing Ca^{2+} and Mg^{2+}, cells were exposed to 0.5 mg/ml of a membrane-impermeable biotinylation reagent (sulfo-NHS-LC-LC-biotin; Pierce) at 4 °C for 15 min. The reaction was quenched by adding 1 ml of culture medium, and then cell extracts were prepared with 0.35 ml of PBS containing 1% Nonidet P-40, 2 mM EDTA, and a protease inhibitor mix (Roche Applied Science). After centrifugation at 12,000 × *g* for 5 min, the supernatants obtained were incubated with immobilized streptavidin-agarose at 4 °C for 1 h. The agarose was washed three times with PBS containing 1% Nonidet P-40, 2 mM EDTA, and subsequently biotinylated proteins were eluted from the agarose by incubating with 5 mg/ml of a water-soluble biotin derivative (sulfo-NHS-biotin; Pierce) dissolved in a buffer (50 mM Tris, pH 8, 150 mM NaCl, 5 mM EDTA, 0.5% Nonidet P-40). The supernatant obtained was subjected to SDS-PAGE followed by Western blot analyzes.

Immunoprecipitation—HEK293 cells (2–5 × 10^7 cells) stably expressing mouse CD14, EIAV-tagged mouse TLR4, FLAG-tagged mouse TLR4, and either EIAV-tagged mouse MD-2 or EIAV-tagged mouse MD-2-T57A,V61A,E122A were suspended into 1 ml of culture medium. After stimulation with compound 506 or lipid IVa, cells were washed with cold PBS, and cell extracts were prepared with PBS containing 0.5% Nonidet P-40, 1 μM okadaic acid, and a protease inhibitor mix (Roche Applied Science). To the cell extracts, anti-FLAG M2-agarose (Sigma) was added, and the mixture was incubated at 4 °C for 1 h. The agarose was washed three times with PBS containing 0.5% Nonidet P-40, and subsequently bound proteins were eluted from the agarose by incubating with an elution buffer (0.1 M glycine, pH 3.5, 0.5% Nonidet P-40). The supernatant obtained was subjected to SDS-PAGE followed by Western blot analyses.

RESULTS

Responsiveness to Lipid A Molecules in HEK293 Cells Expressing CD14, TLR4, and MD-2—We first attempted to confirm the involvement of MD-2 in the animal species-specific activity of lipid IVa in HEK293 cells, which only respond to lipid A for the activation of NF-κB when CD14, TLR4, and MD-2 molecules are present. In HEK293 cells transiently expressing mouse CD14, TLR4, and MD-2, both compound 506 and lipid IVa comparably stimulated the NF-κB-dependent reporter activity (Fig. 1*A*). When mouse MD-2 was replaced with human MD-2, compound 506 still actively stimulated cells, whereas the response to lipid IVa was substantially impaired (Fig. 1*B*).

To examine the antagonistic activity of lipid IVa, HEK293 cells expressing mouse CD14, TLR4, and either mouse MD-2 or human MD-2 were stimulated with compound 506 in the presence of increasing concentrations of lipid IVa (Fig. 2). In cells expressing mouse MD-2, NF-κB-dependent reporter activity stimulated with 10 ng/ml compound 506 was almost unaffected by lipid IVa. In contrast, when mouse MD-2 was replaced with human MD-2, lipid IVa inhibited the compound 506-induced activation of NF-κB in a concentration-dependent

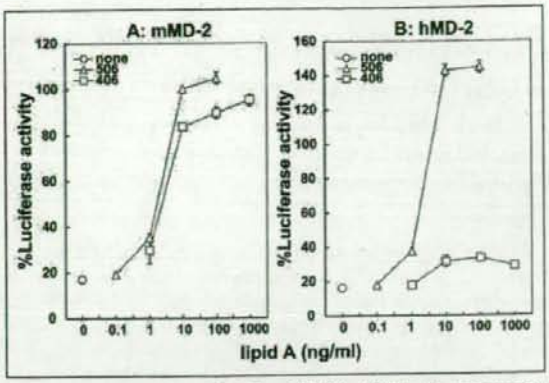

FIGURE 1. **Agonistic activities of lipid A and lipid IVa.** HEK293 cells were transiently transfected with mouse CD14, mouse TLR4, and either mouse MD-2 (*A*) or human MD-2 (*B*) expression plasmids together with an NF-κB-dependent luciferase reporter plasmid. After 24 h, cells were either unstimulated (○) or stimulated for 6 h with indicated concentrations of compound 506 (△) or lipid IVa (□), and luciferase activity was measured. The activity obtained with 10 ng/ml compound 506 in cells expressing mouse CD14, mouse TLR4, and mouse MD-2 was defined as 100%. Values are the means ± S.E. from seven independent experiments.

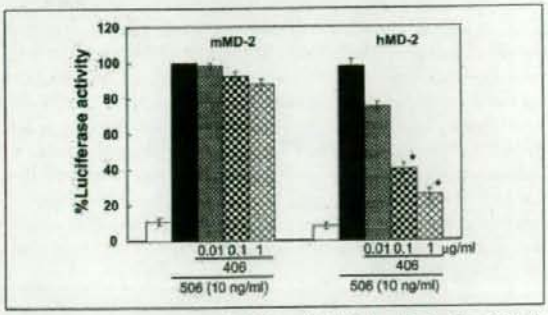

FIGURE 2. **Antagonistic activity of lipid IVa on lipid A-induced activation of NF-κB.** HEK293 cells were transiently transfected with mouse CD14, mouse TLR4, and either mouse MD-2 (*left five columns*) or human MD-2 (*right five columns*) expression plasmids together with an NF-κB-dependent luciferase reporter plasmid. After 24 h, cells were either unstimulated (*open columns*) or stimulated for 6 h with 10 ng/ml compound 506 (*506*) in the absence or presence of indicated concentrations of lipid IVa (*406*), and luciferase activity was measured. The activity obtained with 10 ng/ml compound 506 in cells expressing mouse CD14, mouse TLR4, and mouse MD-2 was defined as 100%. Values are the means ± S.E. from four independent experiments. * $p < 0.01$ (compared with the respective response in the absence of lipid IVa by two-tailed Student's *t* test).

manner. These results indicate that the difference in MD-2 structure between human and mouse is involved in determining the agonist-antagonist activity of lipid IVa.

MD-2 Structural Region Involved in Determining Agonist-Antagonist Activity of Lipid IVa—To explore the MD-2 structure required for the agonist-antagonist activity of lipid IVa, the coding region of mouse MD-2 was divided into six regions, and a series of MD-2 mutant plasmids in which each region was replaced with corresponding human MD-2 sequence was created (Fig. 3*A*). These chimeric mutants were expressed in HEK293 cells together with mouse CD14 and TLR4, and the NF-κB-dependent reporter activity was investigated (Fig. 3*B*). The cell surface expression of each of these MD-2 mutants was confirmed by Western blotting of biotinylated cell surface proteins, indicating that each of these mutants was similar enough to the parental mouse protein to be delivered to the cell membrane (Fig. 3*C*). Cells expressing each of the MD-2 mutants responded to compound 506 comparably with slight variations, indicating that all of these mutants functioned properly. In

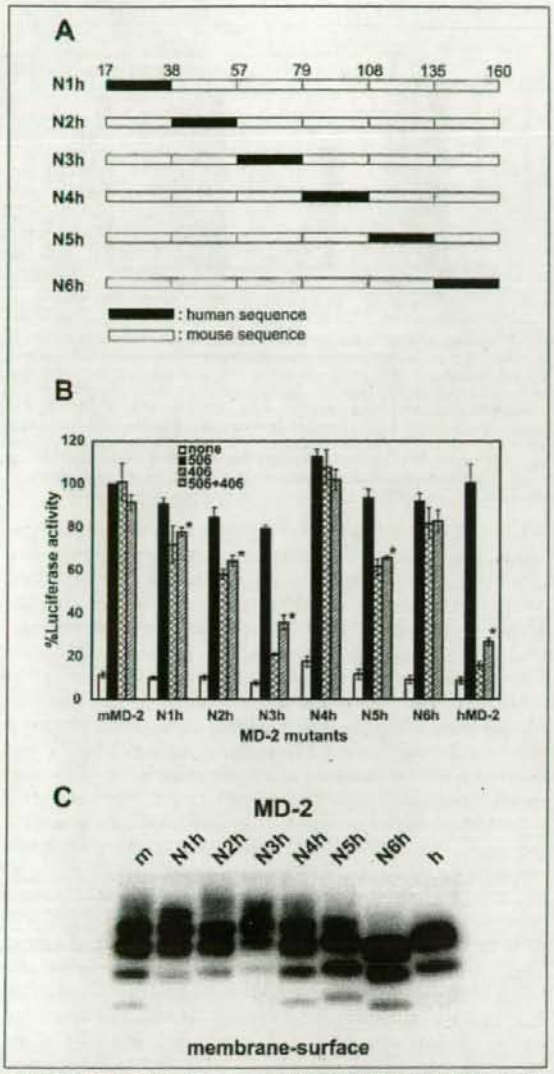

FIGURE 3. **Agonistic and antagonistic activities of lipid IVa in human/mouse chimeric MD-2.** *A*, schematic representation of human/mouse MD-2 constructs. The amino acid sequence of mouse MD-2 was divided into six regions at the indicated amino acid numbers, and each region was replaced with the corresponding human MD-2 sequence. The predicted signal peptide sequence (amino acids 1–16) was omitted. *B*, HEK293 cells were transiently transfected with mouse CD14, mouse TLR4, and the indicated mutant MD-2 expression plasmids together with an NF-κB-dependent luciferase reporter plasmid. After 24 h, cells were either unstimulated (*open columns*) or stimulated for 6 h with 10 ng/ml compound 506 (*506*), 1 μg/ml lipid IVa (*406*), or 10 ng/ml compound 506 in the presence of 1 μg/ml lipid IVa (*506 + 406*), and luciferase activity was measured. The activity obtained with 10 ng/ml compound 506 in cells expressing mouse CD14, mouse TLR4, and mouse MD-2 was defined as 100%. Values are the means ± S.E. from at least four independent experiments. * $p < 0.01$ (compared with the respective response in the absence of lipid IVa by two-tailed Student's *t* test). *C*, HEK293 cells were transiently transfected with mouse CD14, mouse TLR4, and the indicated mutant MD-2 expression plasmids. After 24 h, cell surface proteins were biotinylated with a membrane-impermeable biotinylation reagent, and biotinylated proteins from cell extracts were collected with streptavidin-agarose. After washing, biotinylated proteins were eluted from the agarose by incubating with a water-soluble biotin derivative, and the supernatant obtained was subjected to SDS-PAGE followed by Western blot analysis to detect membrane surface MD-2 mutant proteins. Similar results were obtained in two additional experiments.

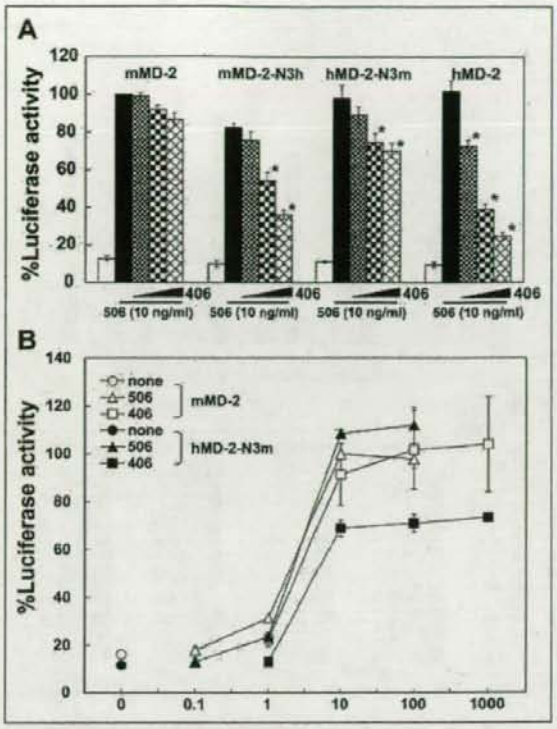

FIGURE 4. **N3 region of MD-2 is partly involved in animal species-specific activity of lipid IVa.** HEK293 cells were transiently transfected with mouse CD14, mouse TLR4, and the indicated mutant MD-2 expression plasmids together with an NF-κB-dependent luciferase reporter plasmid. After 24 h, cells were either unstimulated (*open columns*) or stimulated for 6 h with 10 ng/ml compound 506 (*506*) in the absence or presence of increasing concentrations (0.01, 0.1, and 1 μg/ml) of lipid IVa (*406*) in *A*, or were either unstimulated (○, ●) or stimulated for 6 h with the indicated concentrations of compound 506 (△, ▲) or lipid IVa (□, ■) in *B*, and luciferase activity was measured. The activity obtained with 10 ng/ml compound 506 in cells expressing mouse CD14, mouse TLR4, and mouse MD-2 was defined as 100%, and luciferase activity was measured. The activity obtained with 10 ng/ml compound 506 in cells expressing mouse CD14, mouse TLR4, and mouse MD-2 was defined as 100%. Values are the means ± S.E. from at least three independent experiments. * $p < 0.01$ (compared with the respective response in the absence of lipid IVa by two-tailed Student's *t* test).

contrast, the activity of lipid IVa varied and was substantially impaired in cells expressing the mMD-2-N3h mutant. The activity was similar to that observed in cells expressing human MD-2. A partial reduction with a statistical significance in the activity of lipid IVa was also observed in mMD-2-N2h and mMD-2-N5h mutants as well as in mMD-2-N1h to a lesser extent. The antagonistic activity of lipid IVa was also studied in these MD-2 mutants by stimulating with compound 506 in the presence of lipid IVa. (Fig. 3*B*). In cells expressing mouse MD-2, lipid IVa did not inhibit the compound 506-induced activation of NF-κB, whereas in cells expressing human MD-2 the activity of compound 506 was inhibited substantially by lipid IVa as mentioned above. When MD-2 mutants were expressed, the activity of compound 506 was inhibited by lipid IVa in cells expressing the mMD-2-N3h mutant to a degree similar to that observed with human MD-2. These results suggest that the N3 region of MD-2 is involved in the animal species-specific activity of lipid IVa.

We next asked whether the N3 region of MD-2 is critical for establishing the agonist-antagonist activity of lipid IVa. To address this, HEK293 cells expressing mouse CD14, TLR4, and N3 chimeras or

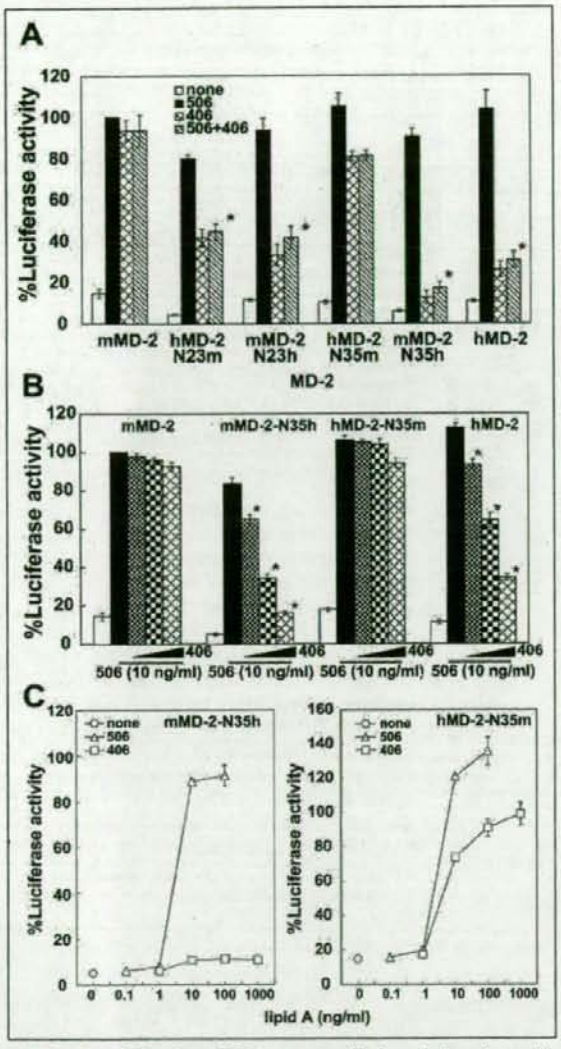

FIGURE 5. **N3 and N5 regions of MD-2 are responsible for animal species-specific activity of lipid IVa.** HEK293 cells were transiently transfected with mouse CD14, mouse TLR4, and the indicated mutant MD-2 expression plasmids together with an NF-κB-dependent luciferase reporter plasmid. After 24 h, cells were either unstimulated (*open columns*) or stimulated for 6 h with 10 ng/ml compound 506 (*506*), 1 μg/ml lipid IVa (*406*), or 10 ng/ml compound 506 in the presence of 1 μg/ml of lipid IVa (*506 + 406*) in *A*, or were either unstimulated (*open columns*) or stimulated for 6 h with 10 ng/ml compound 506 in the absence or presence of increasing concentrations (0.01, 0.1, and 1 μg/ml) of lipid IVa in *B*, or were either unstimulated (○) or stimulated for 6 h with the indicated concentrations of compound 506 (△) or lipid IVa (□) in *C*, and luciferase activity was measured. The activity obtained with 10 ng/ml compound 506 in cells expressing mouse CD14, mouse TLR4, and mouse MD-2 was defined as 100%. Values are the means ± S.E. from at least three independent experiments. * $p < 0.01$ (compared with the respective response in the absence of lipid IVa by two-tailed Student's *t* test).

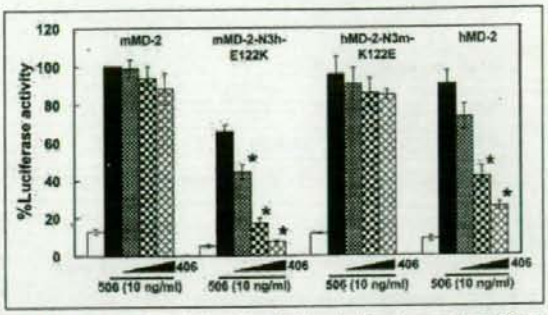

FIGURE 6. **Amino acid 122 of MD-2 is involved in animal species-specific activity of lipid IVa.** HEK293 cells were transiently transfected with mouse CD14, mouse TLR4, and the indicated mutant MD-2 expression plasmids together with an NF-κB-dependent luciferase reporter plasmid. After 24 h, cells were either unstimulated (*open columns*) or stimulated for 6 h with 10 ng/ml compound 506 (*506*) in the absence or presence of increasing concentrations (0.01, 0.1, and 1 μg/ml) of lipid IVa (*406*), and luciferase activity was measured. The activity obtained with 10 ng/ml compound 506 in cells expressing mouse CD14, mouse TLR4, and mouse MD-2 was defined as 100%. Values are the means ± S.E. from at least three independent experiments. * $p < 0.01$ (compared with the respective response in the absence of lipid IVa by two-tailed Student's *t* test).

parental MD-2 were stimulated with compound 506 in the presence of increasing concentrations of lipid IVa (Fig. 4*A*). As expected, lipid IVa concentration-dependently inhibited the compound 506-induced activation of NF-κB in cells expressing the N3h mutant; however, the inhibitory activity was relatively weaker than that observed in cells expressing the parental hMD-2. If the N3 region of MD-2 is the only region responsible for the species-specific activity of lipid IVa, it was expected that replacing the N3 region of human MD-2 with the corresponding mouse MD-2 sequence would show the mouse phenotype. However, a slight inhibitory effect of lipid IVa was still observed in cells expressing the N3m chimera (hMD-2-N3m). In addition, the agonistic activity of lipid IVa in cells expressing this N3m chimera only reached ~73% of the activity observed in cells expressing the parental mouse MD-2 (Fig. 4*B*).

The above result brought us to explore another MD-2 region, in addition to the N3 region, that is involved in the agonist-antagonist activity of lipid IVa. Because a slight antagonistic activity of lipid IVa was observed in mMD-2-N2h and mMD-2-N5h mutants (Fig. 3*B*), we created MD-2 mutant plasmids in which both the N2 and N3 regions or the N3 and N5 regions were mutated. These MD-2 mutants were used to examine the NF-κB-dependent reporter activity in HEK293 cells expressing mouse CD14, TLR4 (Fig. 5*A*). Compound 506 showed activity comparable with all of these MD-2 mutants. With the MD-2 mutant in which the N2 and N3 regions of human MD-2 were replaced with corresponding mouse sequences (hMD-2-N23m) and the mutant in which the N2 and N3 regions of mouse MD-2 were replaced with corresponding human sequences (mMD-2-N23h), lipid IVa showed partial agonistic and partial antagonistic activities. Contrarily, lipid IVa showed a strong agonistic activity with the MD-2 mutant in which the N3 and N5 regions of human MD-2 were replaced with corresponding mouse sequences (hMD-2-N35m), and almost no agonistic activity of lipid IVa, even at 1 μg/ml, was observed with a mutant in which the N3 and N5 regions of mouse MD-2 were replaced with corresponding human sequences (mMD-2-N35h). The antagonistic activity of lipid IVa was also examined with these mutants (Fig. 5*B*). Almost no antagonistic activity was observed with hMD-2-N35m, and a clear antagonistic activity was observed with mMD-2-N35h. In addition, lipid IVa caused almost no agonistic activity in cells expressing mMD-2-N35h and showed a potent agonistic activity comparable with that observed with wild-type mouse MD-2 (see Fig. 1*A*) in cells expressing hMD-2-N35m (Fig. 5*C*). These results indicate that both of the N3 and N5 regions of MD-2 are involved in determining the agonist-antagonist activity of lipid IVa.

MD-2 Structural Region Involved in Antagonistic Activity of Lipid IVa—Replacement of the N3 and N5 regions of mouse MD-2 with corresponding human sequences changed the activity of lipid IVa from agonistic to antagonistic without affecting the activity of compound

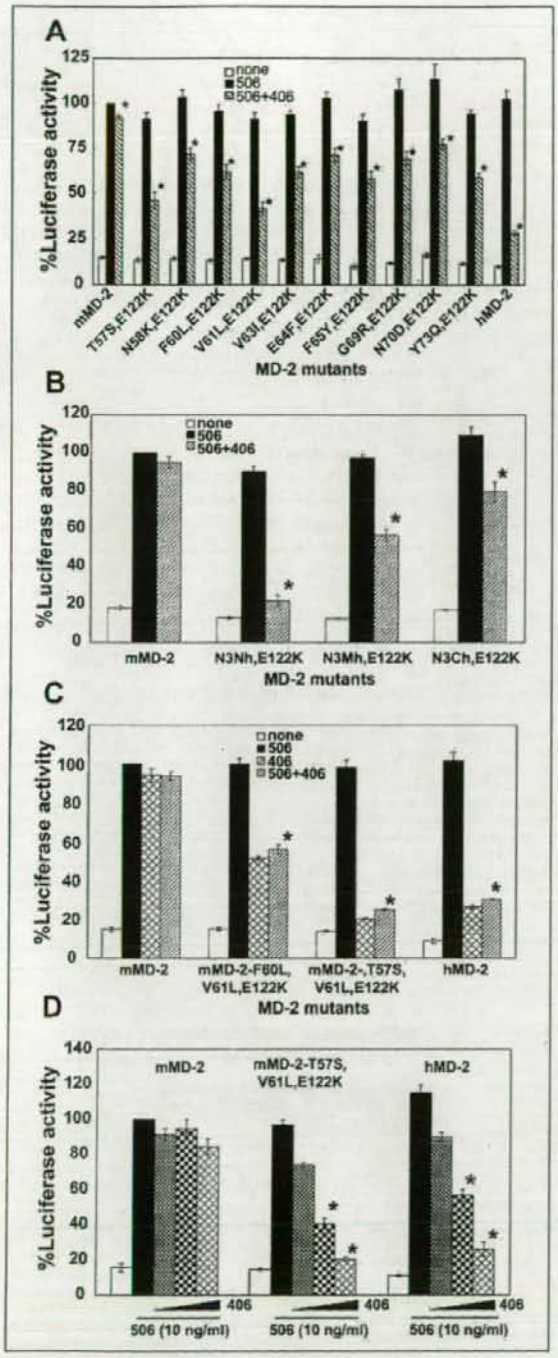

FIGURE 7. **Amino acid residues 57, 61, and 122 of MD-2 are involved in animal species-specific activity of lipid IVa.** HEK293 cells were transiently transfected with mouse CD14, mouse TLR4, and the indicated mutant MD-2 expression plasmids together with an NF-κB-dependent luciferase reporter plasmid. After 24 h, cells were either unstimulated (*open columns*) or stimulated for 6 h with 10 ng/ml compound 506 (*506*) or 10 ng/ml compound 506 in the presence of lipid IVa (*506 + 406*) in *A* and *B*, were either unstimulated (*open columns*) or stimulated for 6 h with 10 ng/ml compound 506, 1 μg/ml lipid IVa, or 10 ng/ml compound 506 in the presence of 1 μg/ml lipid IVa in *C*, or were either unstimulated (*open columns*) or stimulated for 6 h with 10 ng/ml compound 506 in the absence or presence of increasing concentrations (0.01, 0.1, and 1 μg/ml) of lipid IVa in *D*, and luciferase activity was measured. The activity obtained with 10 ng/ml compound 506 in cells expressing mouse CD14, mouse TLR4, and mouse MD-2 was defined as 100%. Values are the means ± S.E. from at least three independent experiments. * $p < 0.01$ (compared with the respective response in the absence of lipid IVa by two-tailed Student's *t* test).

506. Human and mouse MD-2 possess a similar amino acid sequence in their N5 regions with only a major difference at amino acid 122, a change in charge. Thus, to investigate the involvement of amino acid 122 of MD-2 in the activity of lipid IVa, we examined the antagonistic activity of lipid IVa with a mouse MD-2 mutant (mMD-2-N3h-E122K) in which the N3 region and amino acid 122 were replaced with the corresponding human sequence and a human MD-2 mutant (hMD-2-N3m-K122E) in which the N3 region and amino acid 122 were replaced with the corresponding mouse sequence (Fig. 6). A stronger antagonistic activity was observed in cells expressing mMD-2-N3h-E122K compared with those expressing mMD-2-N3h (see Fig. 4). On the other hand, almost no antagonistic effect was observed with hMD-2-N3m-K122E. It is therefore likely that the involvement of the N5 region is explained by amino acid 122.

We next asked whether the involvement of the N3 region was also explained at the amino acid level. To address this, each amino acid of the N3 region of mouse MD-2, carrying E122K mutation, was replaced individually with the corresponding human amino acid residue, and the antagonistic activity of lipid IVa was examined (Fig. 7*A*). Although compound 506-induced activation of NF-κB was inhibited to some extent in cells expressing these MD-2 mutants, sufficient antagonistic activities were not observed. Thus we created mouse MD-2 mutant plasmids in which the overlapping three regions (amino acid residues 57–65, 64–73, and 69–78) within N3 and amino acid 122 were replaced with the corresponding human sequences (each named as N3Nh,E122K, N3Mh,E122K, N3Ch,E122K), and the antagonistic activity of lipid IVa was examined (Fig. 7*B*). A potent antagonistic effect of lipid IVa was observed with the N3Nh,E122K mutant, indicating that amino acid residues 57–65 and 122 of human MD-2 play a role in the antagonistic effect. Because the N3 region of human MD-2 is leucine-rich, we suspected that two leucines (amino acids 60 and 61) might be involved in the antagonistic effect. Thus we created a mouse MD-2 mutant plasmid carrying F60L, V61L, and E122K mutations. Furthermore, because relatively potent antagonistic effects were observed with T57S,E122K and V61L,E122 mutants (Fig. 7*A*), we also created a mouse MD-2 mutant plasmid carrying T57S, V61L, and E122K mutations. Agonistic effects of compound 506 and lipid IVa as well as antagonistic effects of lipid IVa were examined (Fig. 7*C*). Only partial agonistic and antagonistic activities of lipid IVa were observed with the mMD-2-F60L,V61L,E122K mutant. However, these activities and the concentration-inhibition effect of lipid IVa (Fig. 7*D*) in cells expressing the mMD-2-T57S,V61L,E122K mutant were comparable with those observed in hMD-2, indicating a critical role of these three amino acid residues (Ser^{57}, Leu^{61}, and Lys^{122}) for expressing the antagonistic activity.

MD-2 Structural Region Involved in Agonistic Activity of Lipid IVa—Mutation of Thr^{57}, Val^{61}, and Glu^{122} of mouse MD-2 into corresponding human MD-2 sequences caused not only the appearance of antagonistic activity of lipid IVa but also the disappearance of its agonistic activity, without losing the agonistic activity of compound 506 (Fig. 7*C*). Thus we next asked whether these three amino acid residues

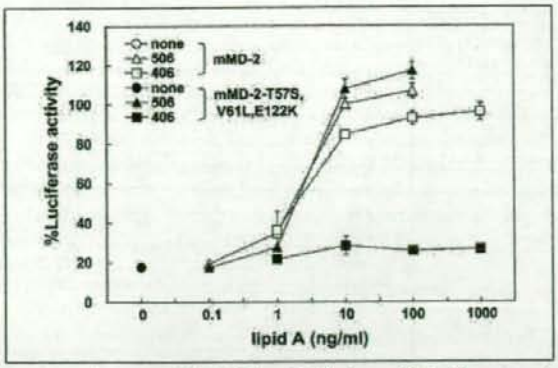

FIGURE 8. **Replacement of Thr^{57}, Val^{61}, and Glu^{122} of mouse MD-2 with corresponding human MD-2 sequence loses the agonistic activity of lipid IVa without affecting lipid A activity.** HEK293 cells were transiently transfected with mouse CD14, mouse TLR4, and the indicated MD-2 expression plasmids together with an NF-κB-dependent luciferase reporter plasmid. After 24 h, cells were either unstimulated (○, ●) or stimulated for 6 h with indicated concentrations of compound 506 (△, ▲) or lipid IVa (□, ■), and luciferase activity was measured. The activity obtained with 10 ng/ml compound 506 in cells expressing mouse CD14, mouse TLR4, and mouse MD-2 was defined as 100%. Values are the means ± S.E. from four independent experiments.

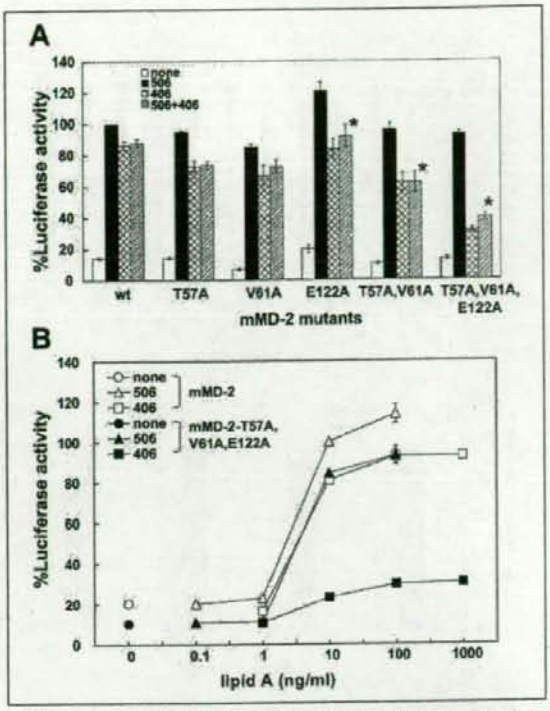

FIGURE 9. **Replacement of Thr^{57}, Val^{61}, and Glu^{122} of mouse MD-2 with alanine loses the agonistic activity of lipid IVa without affecting lipid A activity.** HEK293 cells were transiently transfected with mouse CD14, mouse TLR4, and the indicated MD-2 expression plasmids together with an NF-κB-dependent luciferase reporter plasmid. After 24 h, cells were either unstimulated (*open columns*) or stimulated for 6 h with 10 ng/ml compound 506 (*506*), 1 μg/ml lipid IVa (*406*), or 10 ng/ml compound 506 in the presence of 1 μg/ml lipid IVa (*506 + 406*) in *A*, or were either unstimulated (○, ●) or stimulated for 6 h with the indicated concentrations of compound 506 (△, ▲) or lipid IVa (□, ■) in *B*, and luciferase activity was measured. The activity obtained with 10 ng/ml compound 506 in cells expressing mouse CD14, mouse TLR4, and mouse MD-2 was defined as 100%. Values are the means ± S.E. from three independent experiments. * $p < 0.01$ (compared with the respective response in the absence of lipid IVa by two-tailed Student's *t* test). *wt*, wild-type.

of mouse MD-2 were selectively involved in the agonistic activity of lipid IVa. To address this, we examined the agonistic activities of lipid IVa and compound 506 in cells expressing mMD-2-T57S,V61L,E122K together with mouse CD14 and TLR4 (Fig. 8). In these cells, compound 506 induced potent activation of NF-κB comparable with that observed in cells expressing wild-type mouse MD-2, whereas almost no agonistic activity was observed with lipid IVa at concentrations from 1 to 1,000 ng/ml. Although the mutation of glutamic acid to a lysine caused a charge reversal, mutations from threonine to serine and from valine to leucine may not cause significant changes. It is, therefore, still possible that compound 506 may require these amino acid residues for its agonistic activity, but these changes in amino acid residues may be tolerated. To address this, we mutated these three amino acid residues in mouse MD-2 into alanines either individually or in combinations and examined the agonistic activities of compound 506 and lipid IVa as well as the antagonistic activity of lipid IVa (Fig. 9). Although the agonistic activity of compound 506 with the E122A mutation was slightly enhanced, none of the mutations caused significant changes in the activity of compound 506. No significant changes in the agonistic and antagonistic activities of lipid IVa were observed with each point mutant or the T57S,V61A mutant, whereas the concurrent mutation of all three amino acid residues substantially decreased the agonistic activity, and the antagonistic activity was also evident (Fig. 9*A*). The concentration-response effects showed that the activity of compound 506 was decreased only slightly by the concurrent mutation of all three amino acid residues, whereas the activity of lipid IVa was substantially impaired (Fig. 9*B*). These results indicate that these three amino acid residues are selectively involved in the agonistic activity of lipid IVa and critical for determining its agonist-antagonist activity.

Role of Thr^{57}, Val^{61}, and Glu^{122} of MD-2 in TLR4 Signaling—The role of Thr^{57}, Val^{61}, and Glu^{122} of mouse MD-2 in TLR4 signaling was studied in HEK293 cells stably expressing mouse CD14, EIAV-tagged mouse TLR4, FLAG-tagged mouse TLR4, and either EIAV-tagged mouse MD-2 or EIAV-tagged mouse MD-2-T57A,V61A,E122A. These cells were stimulated with compound 506 or lipid IVa, and TLR4 oligomerization was examined (Fig. 10). For this, FLAG-tagged TLR4 was immunoprecipitated, and coprecipitation of EIAV-tagged TLR4 was detected by Western blotting. Coprecipitations of EIAV-tagged TLR4 were barely detectable without stimulations but were detectable after compound 506 stimulation in both stable transfectants. After lipid IVa stimulation, the coprecipitation was also detected in cells expressing wild-

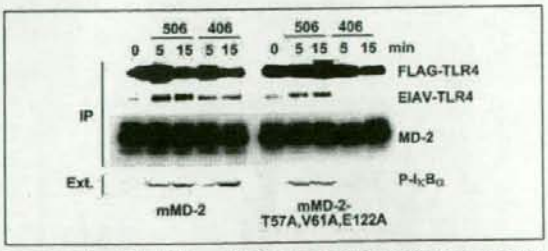

FIGURE 10. **Role of Thr^{57}, Val^{61}, and Glu^{122} of mouse MD-2 in TLR4 signaling.** HEK293 cells stably expressing mouse CD14, EIAV-tagged mouse TLR4, FLAG-tagged mouse TLR4, and either EIAV-tagged mouse MD-2 (*left five lanes*) or EIAV-tagged mouse MD-2-T57A,V61A,E122A (*right five lanes*) were stimulated with 100 ng/ml compound 506 or 1 μg/ml lipid IVa for the indicated times. Then, cell extracts (*Ext.*) were prepared, and FLAG-tagged TLR4 was immunoprecipitated (*IP*). Precipitated FLAG-tagged TLR4 and coprecipitated EIAV-tagged TLR4 as well as MD-2 proteins were detected by Western blotting. A part of cell extracts prepared above were subjected to the detection of IκBα protein phosphorylated at Ser^{32}-Ser^{36} (*P-IκBα*) by Western blotting. Similar results were obtained in two additional experiments.

type MD-2 but was barely detectable in cells expressing mMD-2-T57A,V61A,E122A. Both the wild-type and mutant MD-2 were coprecipitated with TLR4 without ligand stimulation, and the amount coprecipitated was unaffected by stimulations. In parallel with TLR4 oligomerization, the inducible phosphorylation of IκBα was observed in response to compound 506 in both stable transfectants. The phosphorylation was also observed in response to lipid IVa in cells expressing wild-type MD-2 but was barely detectable in cells expressing mMD-2-T57A,V61A,E122A. These results support the above conclusion that Thr^{57}, Val^{61}, and Glu^{122} of mouse MD-2 are selectively involved in the agonistic activity of lipid IVa and critical for determining its agonist-antagonist activity.

DISCUSSION

In the present study, we investigated the structural region of MD-2 required for agonistic and antagonistic activities of lipid IVa by utilizing its animal species-specific activity. The involvement of MD-2 in animal species-specific activity of lipid IVa has been demonstrated previously by expressing human and mouse MD-2 in human monocytic THP-1 cells (4), mouse pro B Ba/F3 cells (15), and HEK293 cells (17). In the present study, we confirmed that the lipid IVa-induced activation of NF-κB in HEK293 cells expressing mouse CD14, TLR4, and MD-2 was substantially impaired when mouse MD-2 was replaced with human MD-2. The activity of compound 506, a typical lipid A molecule, was not significantly affected by the replacement, indicating that both human and mouse MD-2 are functional on mouse TLR4. Thus, in the present study, we created mouse/human chimeric MD-2 mutant plasmids and found that both the N3 (amino acids 57–79) and N5 (amino acids 108–135) regions of MD-2 were involved in the species-specific activity of lipid IVa. We further narrowed the region down and found that the concurrent replacement of Thr^{57}, Val^{61}, and Glu^{122} of mouse MD-2 with the corresponding human MD-2 amino acids substantially decreased the agonistic activity of lipid IVa without affecting the activity of compound 506. The replacement of each of these amino acid residues individually or as pairs was not enough to lose the activity, indicating that these three residues together contribute to the species-specific activity of lipid IVa. A tertiary structure model of human MD-2, reported by Gruber *et al.* (20), shows that amino acid residues 57, 61, and 122 of MD-2 are sterically located in close proximity. Thus the domain created by these three amino acid residues may be involved in determining the agonist-antagonist activity of lipid IVa.

The mutation of Thr^{57} to Ser, Val^{61} to Leu, and Glu^{122} to Lys of mouse MD-2 substantially decreased the agonistic activity of lipid IVa, whereas these replacements did not affect the activity of compound 506. Because the difference in amino acid structure between Thr and Ser or between Val and Leu is only one methyl or methylene moiety, there was still the possibility that these changes in amino acid residues may be tolerated even though compound 506 may require these amino acid residues for full agonistic activity. Thus we examined the activity of compound 506 in a mouse MD-2 mutant in which Thr^{57}, Val^{61}, and Glu^{122} were replaced with alanines, and we found that the activity was not affected by these substitutions, whereas the activity of lipid IVa was substantially impaired. It is therefore likely that these three amino acid residues are selectively involved in the agonistic activity of lipid IVa.

The replacement of amino acid residues 57, 61, and 122 of mouse MD-2 with corresponding human MD-2 amino acids substantially decreased the agonistic activity of lipid IVa. However, replacement of amino acid residues 57, 61, and 122 of human MD-2 with the corresponding mouse MD-2 amino acid residues restored the agonistic activity of lipid IVa only to ~50% of the activity observed in mouse MD-2 (data not shown). Replacement of the N3 region, and replacement of amino acid 122 in addition to the N3 region of human MD-2 with corresponding mouse MD-2 sequence restored the activity to ~73% (Fig. 4*B*) and 90% (data not shown), respectively. Therefore, these three amino acid residues are necessary for the agonistic activity of lipid IVa, but additional amino acid residues in the N3 region may be required for its full agonistic activity.

It has been reported, in studies using soluble MD-2 (6, 21–23) and a peptide fragment of MD-2 (24) that LPS directly binds to MD-2 in a highly basic region (amino acids 119–132). In our study, the mutation of Thr^{57}, Val^{61}, and Glu^{122} of mouse MD-2 to alanines (Fig. 9) or the mutation of Ser^{57}, Leu^{61}, and Lys^{122} of human MD-2 to corresponding mouse MD-2 amino acid residues (data not shown) did not affect the agonistic activity of compound 506, indicating that these three amino acid residues are not involved in lipid A binding. In addition, it is unlikely that these three amino acid residues are involved in lipid IVa binding because lipid IVa showed an antagonistic effect in cells expressing the mouse MD-2 mutant in which all three of these amino acid residues were replaced with the corresponding human MD-2 amino acid residues or with alanines. For TLR4 signaling, the interaction between MD-2 and TLR4 (7, 22, 23, 25), as well as dimerization of TLR4 (26, 27) were reported to be important. For the interaction with TLR4, Cys^{95}, Tyr^{102}, and Cys^{105} of human MD-2 have been reported to be involved (22–23, 25). Miyake (5) and Gangloff and Gay (28) have proposed that MD-2 plays an important role in regulating TLR4 dimerization upon LPS binding. Because the ability of MD-2 to associate with TLR4 and compound 506-induced TLR4 dimerization as well as inducible phosphorylation of IκBα were not affected by the mutation of Thr^{57}, Val^{61}, and Glu^{122} of mouse MD-2 (Fig. 10), these amino acid residues are unlikely to be involved in interactions with TLR4 or in TLR4 dimerization. These amino acid residues may participate in the discrimination of lipid A structure.

Acknowledgments—We thank Keisuke Nakada and Takamasa Hiratsuka for technical assistance.

REFERENCES

1. Schletter, J., Heine, H., Ulmer, A. J., and Rietschel, E. T. (1995) *Arch. Microbiol.* **164,** 383–389
2. Ulevitch, R. J., and Tobias, P. S. (1995) *Annu. Rev. Immunol.* **13,** 437–457
3. Hatada, E. N., Krappmann, D., and Scheidereit, C. (2000) *Curr. Opin. Immunol.* **12,** 52–58
4. Fujihara, M., Muroi, M., Tanamoto, K., Suzuki, T., Azuma, H., and Ikeda, H. (2003) *Pharmacol. Ther.* **100,** 171–194
5. Miyake, K. (2004) *Trends Microbiol.* **12,** 186–192
6. Gioannini, T. L., Teghanemt, A., Zhang, D., Coussens, N. P., Dockstader, W., Ramaswamy, S., and Weiss, J. P. (2004) *Proc. Natl. Acad. Sci. U. S. A.* **101,** 4186–4191
7. Nagai, Y., Akashi, S., Nagafuku, M., Ogata, M., Iwakura, Y., Akira, S., Kitamura, T., Kosugi, A., Kimoto, M., and Miyake, K. (2002) *Nat. Immunol.* **3,** 667–672
8. da Silva, C. J., and Ulevitch, R. J. (2002) *J. Biol. Chem.* **277,** 1845–1854
9. Ohnishi, T., Muroi, M., and Tanamoto, K. (2003) *Clin. Diagn. Lab. Immunol.* **10,** 405–410
10. Lüderitz, O., Freudenberg, M., Galanos, C., Lehmann, E. T., Rietschel, E. T., and Shaw, D. H. (1982) *Curr. Top Membr. Transp.* **17,** 79–151
11. Tanamoto, K., and Azumi, S. (2000) *J. Immunol.* **164,** 3149–3156
12. Means, T. K., Golenbock, D. T., and Fenton, M. J. (2000) *Cytokine Growth Factor Rev.* **11,** 219–232
13. Poltorak, A., Ricciardi-Castagnoli, P., Citterio, S., and Beutler, B. (2000) *Proc. Natl. Acad. Sci. U. S. A.* **97,** 2163–2167
14. Lien, E., Means, T. K., Heine, H., Yoshimura, A., Kusumoto, S., Fukase, K., Fenton, M. J., Oikawa, M., Qureshi, N., Monks, B., Finberg, R. W., Ingalls, R. R., and Golenbock, D. T. (2000) *J. Clin. Invest.* **105,** 497–504
15. Akashi, S., Nagai, Y., Ogata, H., Oikawa, M., Fukase, K., Kusumoto, S., Kawasaki, K., Nishijima, M., Hayashi, S., Kimoto, M., and Miyake, K. (2001) *Int. Immunol.* **13,**

1595–1599
16. Muroi, M., Ohnishi, T., and Tanamoto, K. (2002) *Infect. Immun.* **70,** 3546–3550
17. Hajjar, A. M., Ernst, R. K., Tsai, J. H., Wilson, C. B., and Miller, S. I. (2002) *Nat. Immunol.* **3,** 354–359
18. Muroi, M., and Tanamoto, K. (2002) *Infect. Immun.* **70,** 6043–6047
19. Muroi, M., Ohnishi, T., and Tanamoto, K. (2002) *J. Biol. Chem.* **277,** 42372–42379
20. Gruber, A., Manèek, M., Wagner, H., Kirschning, C. J., and Jerala, R. (2004) *J. Biol. Chem.* **279,** 28475–28482
21. Viriyakosol, S., Tobias, P. S., Kitchens, R. L., and Kirkland, T. N. (2001) *J. Biol. Chem.* **276,** 38044–38051
22. Visintin, A., Latz, E., Monks, B. G., Espevik, T., and Golenbock, D. T. (2003) *J. Biol. Chem.* **278,** 48313–48320
23. Re, F., and Strominger, J. L. (2003) *J. Immunol.* **171,** 5272–5276
24. Manèek, M., Pristovšek, P., and Jerala, R. (2002) *Biochem. Biophys. Res. Commun.* **292,** 880–885
25. Kawasaki, K., Nogawa, H., and Nishijima, M. (2003) *J. Immunol.* **170,** 413–420
26. Medzhitov, R., Preston-Hurlburt, P., and Janeway, C. A. J. (1997) *Nature* **388,** 394–397
27. Zhang, H., Tay, P. N., Cao, W., Li, W., and Lu, J. (2002) *FEBS Lett.* **532,** 171–176
28. Gangloff, M., and Gay, N. J. (2004) *Trends Biochem. Sci.* **29,** 294–300

Food Additives and Contaminants, February 2006; 23(2): 212–218

Taylor & Francis
Taylor & Francis Group

Migration of formaldehyde and acetaldehyde into mineral water in polyethylene terephthalate (PET) bottles

M. MUTSUGA, Y. KAWAMURA, Y. SUGITA-KONISHI, Y. HARA-KUDO, K. TAKATORI, & K. TANAMOTO

National Institute of Health Sciences, Tokyo, Japan

(Received 10 May 2005; revised 14 September 2005; accepted 6 October 2005)

Abstract
The levels of formaldehyde (FA) and acetaldehyde (AA) in polyethylene terephthalate (PET) bottles and in commercial mineral water are reported. All the water samples bottled in Japan contained detectable levels of FA (10.1–27.9 $\mu g l^{-1}$) and AA (44.3–107.8 $\mu g l^{-1}$). Of 11 European bottled water samples, eight did not contain either FA or AA, while the remaining three had detectable levels of FA (7.4–13.7 $\mu g l^{-1}$) and AA (35.9–46.9 $\mu g l^{-1}$). In three North American bottled water samples, two contained FA (13.6 and 19.5 $\mu g l^{-1}$) and AA (41.4 and 44.8 $\mu g l^{-1}$), and one did not. Regardless of the region of origin, all the sterilized water samples contained FA and AA, whilst in contrast, none of the unsterilized water without carbonate contained FA or AA. Of the carbonated water samples, three contained FA and AA, and one did not. When fortified with FA and AA, the commercial water sample without otherwise detectable FA and AA was able to reduce levels, although the commercial water sample containing FA and AA could not. The presence of bacteria in the commercial water samples was investigated using an ATP-based bioluminescent assay and heterotrophic plate count method. The commercial water without FA and AA contained heterotrophic bacteria, whilst the commercial water with FA and AA did not contain detectable bacteria. It is suggested that in this case both FA and AA migrated from PET materials, but were subsequently decomposed by the heterotrophic bacteria in the unsterilized water.

Keywords: *Polyethylene terephthalate (PET), commercial mineral water, formaldehyde, acetaldehyde, heterotrophic bacteria.*

Introduction

Acetaldehyde (AA) has been reported as being present in polyethylene terephthalate (PET) bottles (Dong et al. 1980; Wyatt 1983; Duflos et al. 1993; Linssen et al. 1995) and bottled mineral water (Nijssen et al. 1996; Sugaya et al. 2001; Dabrowska et al. 2002; Nawrocki et al. 2002; Ewender et al. 2003; Hirayama et al. 2003). AA was reported to migrate from the PET plastics, resulting in an undesirable slightly sweet and fruity taste in the mineral water, particularly in the case of carbonated mineral water (Nijssen et al. 1996; Dabrowska et al. 2002; Nawrocki et al. 2002). On the other hand, there are only a few reports of formaldehyde (FA) in PET bottles and bottled water (Villain et al. 1994; Sugaya et al. 2001; Ewender et al. 2003; Hirayama et al. 2003).

The determination of the AA content of PET is generally carried out using headspace gas chromatography (HS/GC). In contrast, the determination of FA in PET samples using HS/GC is difficult because FA is generated by the heating of PET in the headspace sample. Previous papers reported an analytical method for FA and AA in PET products (Mutsuga et al. 2003). In this method, the PET samples are not heated, allowing the accurate measurement of free FA without decomposition of the PET samples. The levels of FA and AA were measured in PET products including bottles for mineral water (Mutsuga et al. 2005). The findings were that most of the PET products contain FA to the same extent as AA.

In the present study, the content of FA and AA in PET bottled commercial water and the bottle material were determined, and subsequently the origin

Correspondence: M. Mutsuga, National Institute of Health Sciences, 1-18-1 Kamiyoga, Setagaya-ku, Tokyo, Japan. E-mail: mutsuga@nihs.go.jp

ISSN 0265-203X print/ISSN 1464-5122 online
DOI: 10.1080/02652030500398361

and disappearance of FA and AA in commercial water was studied.

Materials and methods

Sample

Twenty PET-bottled commercial mineral water samples were purchased in Japan between April 2003 and March 2004; six were bottled in Japan, 11 were bottled in Europe and three were bottled in North America.

Reagents

Formaldehyde solution (37%), hydrochloric acid for precision analysis grade (36%) and sodium sulfate were purchased from Sigma Aldrich Japan (Tokyo, Japan). Acetaldehyde was purchased from Aldrich Chemical Co., Inc. (Milwawkee, WI, USA). 2,4-Dinitrophenylhydrazine (DNPH) hydrochloride for HPLC labelling grade, formaldehyde 2,4-dinitrophenylhydrazone (FA-DNPH) and acetaldehyde 2,4-dinitrophenylhydrazone (AA-DNPH) were purchased from Tokyo Kasei Kogyo Co, Ltd (Tokyo, Japan). Trifluoroacetic acid, potassium carbonate and dichloromethane for dioxin analysis grade were purchased from Wako Pure Chemical Industries, Ltd (Osaka, Japan). Acetonitrile for high-performance liquid chromatography (HPLC) grade were purchased from Merck Co., Inc. (Darmstadt, Germany). Sterilized water was prepared by autoclaving the commercial mineral water in glass bottles.

The CheckLite-HS kit (ATP-based bioluminescent assay kit, containing luciferin-luciferase reagent, ATP-eliminating reagent (ATPase) and ATP-releasing reagent), and CheckLite ATP standard (ATP standard solutions kit) were purchased from Kikkoman International (Chiba, Japan). The LIVE/DEAD BacLight bacterial viability kit (stains mixture of SYTO 9 and propidium iodide) was purchased from Molecular Probes (Eugene, OR, USA), and R2A agar was purchased from Difco Laboratories (Detroit, MI, USA). The membrane filter (0.45 μm, i.d. 13 mm and 0.22 μm, i.d. 47 mm) used was Millex-LH and contains nitrocellulose (Millipore). The carbon membrane filter (0.2 μm, i.d. 19 mm) used was from Track-Etch Membrane (Whatman, ME, USA).

Apparatus

FA and AA were quantified using an HPLC system consisting of the Shimadzu LC-10A (Shimadzu Co., Kyoto, Japan).

Bioluminescence was measured using a Lumitester C-100N (Kikkoman International). Direct counting of bacteria was performed with an epifluorescence microscopy OLYMPUS BX60 (Olympus Co., Tokyo, Japan).

Preparation of standard solution

Stock solution (100 $\mu g\,ml^{-1}$ each FA and AA) was prepared by dissolving 70.0 mg FA-DNPH and 50.9 mg AA-DNPH in 100 ml acetonitrile. Standard solutions with which to calculate curves were prepared by stepwise dilution with the acetonitrile/water (1:1) ranging in concentration from 0.05 to 5 $\mu g\,ml^{-1}$ for FA and AA.

Analytical procedure for mineral water

Commercial water (100 ml) was collected in 200 ml glass flasks, 5 ml DNPH/hydrochloric acid solution (1 $mg\,ml^{-1}$) added and then derivatized for 2 h at room temperature. Approximately 3.7 g potassium carbonate were added slowly with agitating to adjust the pH to approximately 3. The solution was transferred into a separatory funnel and derivatives extracted with dichloromethane (25 ml × 2). The dichloromethane layers were collected and added about 2 g sodium sulfate and filtrated. The filtrate was evaporated completely under reduced pressure. The residue was dissolved in 2 ml acetonitrile.

Analytical procedure for PET bottle material

PET bottle material (0.5 g) was cut into small pieces and placed in a 5 ml centrifuge glass tube equipped with a glass plug, after which 2.5 ml DNPH/trifluoroacetic acid solution (1 $mg\,ml^{-1}$) was added and the mixture left overnight for dissolution and derivatization. Dichloromethane (10 ml) was then added and approximately 12 ml potassium carbonate solution (0.2 $g\,ml^{-1}$ dissolved in sterilized water) was added to adjust the pH to 7, when the solution changed to a thick yellow liquid. The precipitates were removed by filtration under reduced pressure and washed with dichloromethane (2 × 10 ml). The filtrate and washes were combined and transferred to a separatory funnel. The dichloromethane layers were separated from the aqueous layer, which was subsequently extracted using dichloromethane (10 ml). The dichloromethane layers were collected and dried via the addition of sodium sulfate and evaporation. The residue was dissolved in 2.5 ml acetonitrile and diluted to 5 ml with water, then filtered using a membrane filter (0.45 μm).

HPLC condition

Column: TSKgel ODS-80Ts (4.6 mm i.d. × 250 mm) (Tosoh Co., Tokyo, Japan), guard column: stainless column (1.0 mm i.d. × 45 mm)

packed with ODS (Fuji Silysia Chemical Ltd., Aichi, Japan), flow: 1 ml min^{-1}, column temperature: 50°C, injection volume: 20 µl, mobile phase: 55% acetonitrile/water, detection: UV (360 nm).

Standard aerobic plate count

A water sample (100 ml) was filtered through a membrane filter (0.22 µm) under reduced pressure. The filter was then placed upon a tryptone glucose yeast extract agar medium plate. The plates were incubated aerobically at 37°C for 24 h. Colonies were counted and expressed as colony forming unit (CFU) ml^{-1}.

Direct counting of bacteria with fluorescent staining

A water sample (50 ml) was drawn through a carbon membrane filter under negative pressure. The carbon membrane filter was strained by LIVE/DEAD BacLight bacterial viability kit, 1 ml stains mixture prepared according to the manufacture's instructions, and incubated for 20 min in the dark at room temperature. The mixture was removed and filters mounted with low-fluorescence immersion oil on glass microscope slides and observed by epifluorescence microscopy. The number of green cells was counted after viewing 20 microscopic fields.

ATP-based bioluminescent assay

The ATP derived from bacteria was measured by following methods. A 1 ml aliquot of water sample was placed in a tube, an ATP-eliminating reagent (0.1 ml) was added, the solution was mixed and it was incubated for 10 min to remove any extracellular ATP. A total of 0.1 ml of the solution then combined with 0.1 ml of a detergent for lysing cells before the addition of 0.1 ml luciferin-luciferase reagent. The sample was mixed and the amount of bioluminescence measured using a luminometer. The luminescence curves were prepared using the ATP standard solutions (2×10^{-12}–2×10^{-9} mol ml^{-1}). The results are expressed as relative light units (RLU) and ATP concentration.

Heterotrophic plate counting method

Heterotrophic plate counts (HPC) were obtained by plating 100 µl of tenfold dilutions of commercial water samples on R2A agar plates. The plates were incubated aerobically at 22°C for 72 h. Colonies were counted and the arithmetic mean expressed as CFU ml^{-1}.

Result

Analytical procedure

FA and AA in the PET bottle material were measured as described (Mutsuga et al. 2003, 2005). Recoveries of 76.9–101.2% were obtained for a PET pellet sample (0.5 g) spiked with FA (2.5 µg) and AA (2.5 µg). The limits of detection of FA and AA were 0.2 µg g^{-1} for each, based on the linearity of the calibration curve.

The analytical method for FA and AA in the commercial water was improved upon, and recovery rates of 85.7–104.9% were obtained for sterilized water (100 ml) spiked with FA and AA (1 and 10 µg each). The limit of detection of FA and AA were 5.0 µg l^{-1} for each, based on three times the blank value (FA: 1.34 ± 0.11 µg l^{-1} and AA: 0.77 ± 0.04 µg l^{-1}).

Contents of FA and AA in mineral water

The levels of FA and AA in the 20 commercial water samples are shown in Table I. FA and AA ranged from not detected (n.d.) to 27.9 µg l^{-1} and n.d. to 107.8 µg l^{-1}, respectively. All samples bottled in Japan had detectable levels of FA (10.1–27.9 µg l^{-1}) and AA (44.3–107.8 µg l^{-1}). In the European water, three samples had detectable levels of FA (7.8–13.7 µg l^{-1}) and AA (37.2–46.9 µg l^{-1}), while the remaining eight did not. In the North American water, two samples contained FA (13.6 and 19.5 µg l^{-1}) and AA (41.4 and 44.8 µg l^{-1}), while one did not. Most of the samples bottled in Europe and North America contained FA and AA under the detection limits. The detected levels of FA and AA in the Japanese water were higher than in the European or North American samples. There was no relationship between FA-and-AA content and pH or hardness of the commercial water. The samples were classified into two groups: those in which FA and AA were detected in the water (group A), those in which FA and AA were not detected in the water (group B). Group A contained all the sterilized water samples and three carbonated water samples. Group B contained unsterilized water samples without carbonate and one carbonated water sample.

Content of FA and AA in the bottle material and their migration

The levels of FA and AA in the bottle materials were analysed (Table I). The FA and AA levels of the Japanese bottles ranged from 1.3 to 2.9 µg g^{-1} and from 11.5 to 25.0 µg g^{-1}, respectively, while the European and North American bottles ranged from n.d. to 1.6 µg g^{-1} and from 5.2 to 17.1 µg g^{-1}, respectively. The levels of FA and AA in the Japanese bottles were significantly higher than that in European and North American bottles. The explanation for this may be the higher moulding temperatures used in the production of Japanese bottles (thicker bottle walls) and the use of scavengers in European bottles, which minimizes the

Table I. Contents of FA and AA in mineral water.

Region	Sample number	Bottled country	Representation				Bottle colour	Bottle material ($\mu g\,g^{-1}$)		Water ($\mu g\,l^{-1}$)		
			pH	Hardness	Sterilized	Carbonate		Formaldehyde	Acetaldehyde	Formaldehyde	Acetaldehyde	Classification
Japan												
	J-1	Japan	7.4	84	sterilized	–	colorless	2.2	16.7	10.1	44.3	group A
	J-2	Japan	8.3	32	sterilized	–	colorless	2.9	12.1	27.9	60.7	group A
	J-3	Japan	–	30	sterilized	–	colorless	1.6	13.6	15.0	41.1	group A
	J-4	Japan	–	99	sterilized	–	colorless	1.3	25.0	10.6	107.8	group A
	J-5	Japan	–	25	sterilized	–	colorless	2.4	14.0	15.4	66.3	group A
	J-6	Japan	7.1	28	sterilized	–	colorless	1.7	11.5	17.6	46.4	group A
Europe												
	E-1	France	7.0	62	not treated	–	pale blue	n.d.	8.8	n.d.	n.d.	group B
	E-2	France	7.3	309	not treated	–	colorless	1.0	5.5	n.d.	n.d.	group B
	E-3	France	7.2	294	not treated	–	colorless	0.7	7.2	n.d.	n.d.	group B
	E-4	France	7.6	628	not treated	–	colorless	0.7	5.4	n.d.	n.d.	group B
	E-5	France	–	201	not treated	carbonated	green	0.9	6.7	n.d.	n.d.	group B
	E-6	Italy	7.8	161	not treated	carbonated	deep blue	0.6	5.2	7.9	37.2	group A
	E-7	Italy	7.5	740	not treated	carbonated	green	0.9	8.4	13.7	37.8	group A
	E-8	Italy	5.8	609	not treated	carbonated	green	0.5	6.7	7.8	46.9	group A
	E-9	Italy	7.8	161	not treated	–	green	1.0	5.7	n.d.	n.d.	group B
	E-10	UK	–	104	not treated	–	colorless	1.6	7.5	n.d.	n.d.	group B
	E-11	UK	7.8	122	not treated	–	colorless	1.1	5.9	n.d.	n.d.	group B
North America												
	A-1	Canada	–	24	sterilized	–	pale blue	0.9	9.8	13.6	41.4	group A
	A-2	Canada	–	1	–	–	deep blue	n.d.	9.2	n.d.	n.d.	group B
	A-3	USA	–	38	sterilized	–	colorless	1.1	17.1	19.5	44.8	group A

–, No description.
Each value is the mean of three trials.
Bottle material n.d. $< 0.2\,\mu g\,g^{-1}$, water n.d. $< 5.0\,\mu g\,L^{-1}$.

Table II. Migration of FA and AA from PET bottles into water at 40°C.

Bottle	Contents in bottle ($\mu g\,g^{-1}$)		Storage days	Migration level ($\mu g\,l^{-1}$)	
	FA	AA		FA	AA
J-1	2.2	16.7	14	42.6	112.0
			30	55.2	169.6
E-1	0.7	5.4	14	11.4	14.5
			30	14.9	21.1

Each value is the mean of four trails

formation of FA and AA. Some of the bottles were blue or green colour. However, the results for the European bottles showed that the colour of bottles did not affect the FA and AA levels.

Migration tests were performed using Japanese (J-1) and European (E-1) bottles, in which J-1 bottle contained FA and AA while the E-1 bottles did not. The bottles were washed with sterilized water, then 100 ml sterilized water added, and stored at 40°C for 14 and 30 days. The analysis showed that migration of FA and AA occurred from both bottles to water (Table II). The migration levels of FA and AA depended on the level in the bottle material and duration of storage. Thus, the FA and AA in commercial water was a result of migration from their PET bottles.

Clarification of the disappearance of FA and AA in commercial water

The E-1 bottle showed migration of FA and AA into the sterilized test water, although the commercial water contained in the E-1 bottle was not contaminated with either FA or AA. Thus, it was speculated that unsterilized water might have some capacity to reduce levels of FA and AA.

Thus, 100 ml commercial water samples were transferred to a 200-ml glass bottle with plastic screw cap. Water samples were fortified with 2 μg FA and 10 μg AA and stored in the dark at 37°C for 48 or 96 h (Figure 1 and Table III). Figure 1 shows the time–response curves of FA and AA in E-1 and J-1 water for 12, 24, 36 and 48 h. In E-1 water, FA and AA reduced quickly and reached the 'blank' level after 48 h incubation, whereas the FA and AA in the J-1 water did not decline. Table III shows the recoveries of fortified FA and AA in several kinds of commercial water. Water of group B was able to reduce spiked FA and AA, while water of group A could not. Two carbonated water (E-6 and E-7) produced a small reduction in FA, and it seemed to be more volatile in carbonated water than still water at 37°C. However, water samples (E-1–3)

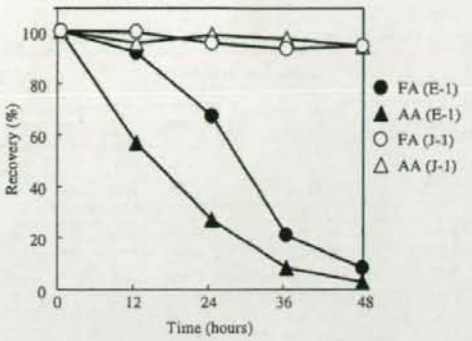

Figure 1. Recovery of FA (2 μg) and of AA (10 μg) fortified to 100 ml E-1 and J-1 water stored at 37°C. Each value is the means of two trials.

Table III. Recoveries of fortified FA and AA in several mineral water samples.

	Sample number	Incubation time (h)	Recovery (%)	
			Formaldehyde	Acetaldehyde
Group A	J-1	48	>95	>95
	J-1	96	>95	>95
	J-3	48	>95	>95
	J-6	48	>95	>95
	E-6	48	78	>95
	E-7	48	83	>95
	A-3	48	95	>95
Group B	E-1	48	<5	<5
	E-2	48	>95	75
	E-2	96	27	<5
	E-3	48	86	5
	E-5	48	>95	10
Sterilized group B	E-1	48	>95	>95
	E-2	96	>95	92
	E-3	48	>95	>95

FA (2 μg) and AA (10 μg) were added to 100 ml mineral water and stored at 37°C for 48 or 96 h.
Each value is the mean of two trials.

after sterilization in group B did not have the same ability to reduce levels.

According to these results, unsterilized commercial water can reduce the levels of FA and AA in the water. It is suspected that bacteria in commercial water were involved in the reduction in FA and AA.

Confirmation of bacterial activity

At first, the standard aerobic plate count method was performed. However, none of the water samples produced colonies. Therefore, the direct counting method was performed using the LIVE/DEAD BacLight bacterial viability kit, which contained two nucleic acid-binding stains, SYTO 9 and propidium iodide (Venkateswaran et al. 2003). SYTO 9 stained

Table IV. Amount of intracellular ATP in water.

Sample number	Bioluminescent assay: Luminescence (RLU)	Bioluminescent assay: ATP ($\times 10^{-11}$ M)	HPC assay colony count (CFU ml^{-1})
Group A			
J-1	n.d.*1	n.d.	n.d.*2
J-2	n.d.	n.d.	–
J-3	n.d.	n.d.	n.d.
J-4	n.d.	n.d.	–
J-5	n.d.	n.d.	–
J-6	n.d.	n.d.	–
E-6	n.d.	n.d.	n.d.
E-7	n.d.	n.d.	–
E-8	n.d.	n.d.	n.d.
A-1	n.d.	n.d.	–
A-3	n.d.	n.d.	–
Group B			
E-1	1005	14.3	1.5×10^5
E-2	149	1.9	3.2×10^4
E-3	801	11.3	7.8×10^4
E-4	655	9.2	–
E-5	1059	15.0	1.6×10^5
E-9	112	1.4	–
E-10	1003	14.2	4.1×10^4
E-11	3808	54.8	–
A-2	778	11.0	–

n.d.*1 < 100 RLU.
n.d.*2 < 100 CFU ml^{-1}.
Each value is the mean of three trials.
–, Not evaluated.

all cells green, while propidium iodide stained all the cells with damaged membranes red. As observed by epifluorescence microscopy, both viable and dead bacteria were detected. In J-1 water, neither green nor red bacteria were detected. On the other hand, in E-1 water, viable green bacteria were visualized (5×10^4 cells ml^{-1}). This bacterium was presumed to heterotrophic bacterium, which exists widely in the environment, as this bacterium is very small and there have been some reports documenting its existence in commercial water (Mosso et al. 1994; Tsai and Yu 1997; Ramalho et al. 2001; Leclerc and Moreau 2002).

Subsequently, intracellular ATP was measured by the ATP-based bioluminescent assay (Table IV). This method confirmed that none of the water samples in group A contained intracellular ATP. On the other hand, the water in group B showed intracellular ATP concentrations of between 1.4×10^{-11} and 5.5×10^{-10} M. Among the carbonated waters, intracellular ATP was detected in E-5 of group B, but not in E-6–8 of group A. All samples showed correlation between the existence of intracellular ATP and a reduction in FA and AA levels.

The enumeration of heterotrophic bacteria in the commercial mineral water is usually performed using the HPC method (Mosso et al. 1994; Tsai and Yu 1997; Ramalho et al. 2001; Leclerc and Moreau 2002; Venkateswaran et al. 2003). This method was recommended by Council Directive 98/83/EC (1998) for the count of heterotrophic bacteria in commercial water, and was performed in the present study on nine water samples by incubation for 72 h at 22°C on R2A medium. None of the water samples in group A possessed heterotrophic bacteria, while the water samples in group B formed between 1.6×10^3 and 1.5×10^5 CFU ml^{-1}.

Discussion

It has been shown that FA and AA migrated into commercial water from the PET bottle material. In commercial water without bacteria, the levels of migrated FA and AA remain unchanged, whereas in natural mineral water containing heterotrophic bacteria, the migrated FA and AA was decomposed. Of the carbonated water samples, one sample contained bacteria and showed a reduction in FA and AA, while the others had no bacteria and showed no decomposition activity. It was speculated that the existence of bacteria influenced the concentration of carbonate gas.

In the European Union regulations, natural mineral water cannot be treated for the elimination of microorganisms by disinfection or sterilization. The current drinking water guidelines in many European countries are based on recently revised Directive 98/83/EC. The current recommended microbiological standards include HPC limits for private supplies, i.e. no significant increase over normal levels when incubated at 22 and 37°C, and for bottled water within 12 h of bottling, 100 CFU ml^{-1} when incubated at 22°C for 72 h and 20 CFU ml^{-1} when incubated at 37°C for 48 h. In the present study, several European waters contained 1.6×10^3–1.5×10^5 CFU ml^{-1} heterotrophic bacteria. These waters appear to have passed the regulations during the bottling stage, but then bacteria proliferated during transport to Japan.

The potential negative impact to human health from the consumption of treated water containing high HPC levels of bacteria is still being debated. However, until now, no report has documented the decomposition of FA and AA by heterotrophic bacteria. PET bottled commercial water has two problems: the existence of heterotrophic bacteria and the migration of FA and AA, and the close relationship exists between these problems. Thus, it is

necessary to pay sufficient attention to both problems.

References

Council Directive 98/83/EC, on the quality of water intended for human consumption. Official Journal of the European Communities L330:32–54.

Dabrowska A, Borcz A, Nawrocki J. 2002. Aldehyde contamination of mineral water stored in PET bottles. Food Additives and Contaminants 20:1170–1177.

Dong M, DiEdwardo HA, Zitomer F. 1980. Determination of residual acetaldehyde in polyethylene terephthalate bottles, preforms, and resins by automated headspace gas chromatography. Journal of Chromatographic Science 18:242–246.

Duflos J, Leroy C, Gervais B, Dupas G, Bourguignon J, Queguiner G. 1993. Analysis of residual acetaldehyde and formaldehyde in PET via HPLC. Analusis 21:313–317.

Ewender J, Franz R, Mauer A, Welle F. 2003. Determination of the migration of acetaldehyde from PET bottles into non-carbonated and carbonated mineral water. Deutsche Lebensmittel-Rundschau 99:215–221.

Hirayama T, Kashima A, Watanabe T. 2003. Amounts of formaldehyde in tap water and commercially available mineral water. Journal of the Food Hygienics Society of Japan 10:138–144.

Leclerc H, Moreau A. 2002. Microbiological safety of natural mineral water. FEMS Microbiology Reviews 26:207–222.

Linssen J, Reitsma H, Cozijnsen J. 1995. Static headspace gas chromatography of acetaldehyde in aqueous foods and polyethylene terephthalate. Zeitschrift für Lebensmittel-Untersuchung und- Forschung 201:253–255.

Mosso AM, Rosa CM, Vivar C, Medina M. 1994. Heterotrophic bacterial populations in the mineral water of thermal springs in Spain. Journal of Applied Bacteriology 77:370–381.

Mutsuga M, Kawamura Y, Tanamoto K. 2003. Analytical method for formaldehyde, acetaldehyde and PET cyclic oligomers in polyethylene terephthalate products. Japanese Journal of Food Chemistry 10:138–144.

Mutsuga M, Tojima T, Kawamura Y, Tanamoto K. 2005. Survey of formaldehyde, acetaldehyde, and oligomers in polyethylene terephthalate food-packaging materials. Food Additives and Contaminants 22:783–789.

Nawrocki J, Dabrowska A, Borcz A. 2002. Investigation of carbonyl compounds in bottled waters from Poland. Water Research 36:4893–4901.

Nijssen B, Kamperman T, Jetten J. 1996. Acetaldehyde in mineral water stored in polyethylene terephthalate (PET) bottles: Odour threshold and quantification. Packaging Technology and Science 9:175–185.

Ramalho R, Cunha J, Teixeira P, Gibbs AP. 2001. Improved methods for the enumeration of heterotrophic bacteria in bottled mineral water. Journal of Microbiological Methods 44:97–103.

Sugaya N, Nakagawa T, Sakurai K, Morita M, Onodera S. 2001. Analysis of aldehydes in water by head space-GC/MS. Journal of Health Science 47:21–27.

Tsai GJ, Yu SC. 1997. Microbiological evaluation of bottled uncarbonated mineral water in Taiwan. International Journal of Food Microbiology 37:137–143.

Venkateswaran K, Hattori N, La Duc TM, Kern R. 2003. ATP as a biomarker of viable microorganisms in clean-room facilities. Journal of Microbiological Methods 52:367–377.

Villain F, Coudane J, Vert M. 1994. Thermal degradation of poly(ethylene terephthalate) and the estimation of volatile degradation products. Polymer Degradation and Stability 43:431–440.

Wyatt MD. 1983. Semi-automation of head space GC as applied to determination of acetaldehyde in polyethylene terephthalate beverage bottles. Journal of Chromatographic Science 21:508–511.

Note

Identification of the Main Constituents in Sandarac Resin, a Natural Gum Base

(Received August 18, 2005)

Naoki SUGIMOTO[*1,†], Masanori KUROYANAGI[*2], Takashi KATO[*2], Kyoko SATO[*1], Atsuko TADA[*1], Takeshi YAMAZAKI[*1] and Kenichi TANAMOTO[*1]

([*1] National Institute of Health Sciences: 1-18-1, Kamiyoga, Setagaya-ku, Tokyo 158-8501, Japan; [*2] School of Bioresources, Hiroshima Prefectural University: 562, Nanatsuka, Shobara, Hiroshima 727-0023, Japan; [†] Corresponding author)

Sandarac resin, a natural gum base, is described as "a substance composed mainly of sandaracopimaric acid obtained from the secretion of sandarac trees" in the List of Existing Food Additives in Japan. To evaluate its quality as a food additive, the main constituents in a sandarac resin product were investigated. Three constituents were isolated and identified as sandaracopimaric acid, sandaracopimarinol and 4-epidehydroabietic acid by MS and 2D-NMR. Quantification of the main constituent, sandaracopimaric acid, was performed by HPLC and its content in the product was determined to be 11.6%.

Key words: food additive; gum base; sandarac resin; *Tetraclinis articulata*; sandaracopimaric acid

Introduction

Most natural food additives have many constituents, but to date, there have been few investigations on the constituents in most of them. It is necessary for the evaluation of natural food additives to analyze the constituents as completely as possible, since the chemical nature and concentrations of the constituents may differ depending on the extraction and processing methods, and the collection season of the plant of origin. We have been investigating the main and minor constituents in various food additives, for which there are no analytical data and/or reports, in order to develop official analytical methods[1,2].

The List of Existing Food Additives in Japan[3] stipulates that sandarac resin is a natural gum base, which is a substance composed mainly of sandaracopimaric acid (1) obtained from the secretion of sandarac trees. Sandarac tree is *Tetraclinis articulata* (Vahl) Mast., belonging to the Cupressaceae family. It is native to Morocco and is a coniferous tree closely related to arborvitae. The existence of several diterpenoids in the leaves of *T. articulata* has recently been reported[4]. Sandarac resin has been used for many years as a natural resin for artwork. Many reports[5,6] have been published on the characterization and identification of natural resins for painting. It was reported that the dominant component in sandarac resin used for painting is sandaracopimaric acid (1). However, the main constituents of sandarac resin as a food additive have not been clarified. In this study, we identified several constituents of sandarac resin as sandaracopimaric acid (1), sandaracopimarinol (2) and 4-epidehydroabietic acid (3) by MS and 2D-NMR, and quantified the content of the main constituent, sandaracopimaric acid (1), by HPLC.

Materials and Methods

1. *Sample and chemicals*

A sample of sandarac resin product was obtained through the Japan Food Additives Association. Silica gel 60 F_{254} (20 cm×20 cm, Art. 1.05715) (Merck Co., Ltd.) was used for TLC. Silica gel 60N (63-200 μm Cat. No. 37565-79) (Kanto Chemical Co., Inc.) was used for open column chromatography. All chemicals were of reagent grade and were used without further purification.

2. *Spectroscopic analysis*

NMR spectra were recorded on JNM-ECA800 and JNM-ECA500 (800 MHz and 500 MHz) instruments (JEOL Co., Ltd.) with chloroform-*d* ($CDCl_3$) as the solvent. ^{1}H-NMR and ^{13}C-NMR spectra were referenced internally to tetramethylsilane (TMS). Assignments of the proton and carbon signals of all isolated compounds were confirmed by pulse field gradient (PFG) heteronuclear multiple quantum coherence (HMQC), PFG heteronuclear multiple bond connectivity (HMBC), double quantum filtered correlation spectroscopy (DQF-COSY) and nuclear Overhauser effect (NOE) experiments. High-resolution electron impact mass spectrometry (HR-EI-MS) spectra were obtained with a JMS-700 (JEOL) mass spectrometer. Melting points were determined using a MP-S3 apparatus (Yanaco New Science Inc.) without correction.